CLM-P81

This document is intended for publication in a journal, and is made available on the understanding that extracts or references will not be published prior to publication of the original, without the consent of the authors.

CLM-P81

United Kingdom Atomic Energy Authority

RESEARCH GROUP

Preprint

A 100 kV low inductance switch (spark gap) for starting diverting and clamping capacitor discharges

A. E. BISHOP
G. D. EDMONDS

Culham Laboratory,
Culham, Abingdon, Berkshire

1966

UNCLASSIFIED
(Approved for Publication)

CLM - P 81

A 100 kV LOW INDUCTANCE SWITCH (SPARK GAP) FOR STARTING, DIVERTING AND CLAMPING CAPACITOR DISCHARGES

by

A.E. Bishop
G.D. Edmonds

A B S T R A C T

The paper describes the recent development of an accurately triggered (± 5 nsec) spark gap of the 'field distortion' type operating in the swinging cascade mode up to 100 kV.

Developed initially as a switch for 'starting' a high frequency (250 kc/s) capacitor discharge it has also been adapted for 'diverting' and 'clamping' such discharges at current up to 200 kA, and passing up to 20 coulombs per discharge.

The field distortion switch is seen as a versatile switch-type capable of extensive development.

U.K.A.E.A. Research Group,
Culham Laboratory,
Nr Abingdon,
Berks.

August, 1965

C O N T E N T S

1. INTRODUCTION

A shock heated plasma experiment called Tarantula(1) required a current discharge of 1.2 MA rising in 1 μsec from a 100 kV source with an initial rate of current rise 2.5×10^{12} amps/sec. Forty 0.5 μF 100 kV capacitors were individually connected to start-switches of the triggered spark gap type described in 1962(2) and then by separate lengths of cable to a low inductance discharge tube. These start switches have been used successfully since then. However, to obtain a greater rate of rise of current an even lower inductance system would be desirable for future experiments. Analysis of the Tarantula circuit elements showed that the discharge tube inductance could be reduced by subdivision into shorter sections, but it would then be essential to reduce the inductances of the capacitors, switches and cable. Although it has proved just possible to develop a lower inductance cable (70 nH/m as against 125 nH/m) it would still be desirable to reduce the length of each cable from 1.8 m to 0.9 m. This would bring the switches electrically closer together and mounting the switches in a circle as on Tarantula would mean that the overall diameter of the switches could not exceed 25 cm. Furthermore, the spread in the firing times of the first to last switch would have to be half that of the Tarantula switches to avoid the early firing of one switch upsetting the firing of the later ones.

Such a start switch has now been developed, and in the course of the investigations it was found that with small modifications the usefulness of this type of switch could be extended to carry out two further switching functions. One of these is to produce a half sine wave of current (with a frequency of 250 kc/s) by short circuiting the source capacitor and start switch at first current zero. This process is known as 'diverting'. The other function is to produce a long current pulse by short circuiting the inductive load at current maximum. This process is known as 'clamping' or 'crowbarring'. The current and voltage waveforms which result from these switching functions are shown in Fig.1. This paper describes the switches which have been developed for the three switching functions 'starting', 'diverting' and 'clamping'.

2. PRINCIPLES OF DESIGN

The Tarantula start switches had to be designed to plug into the re-entrant termination of a capacitor whose design had already been frozen. Due to the long time required for developments on capacitors only minor modifications which gave rise to a large benefit could be considered. It was therefore decided to alter only the output termination of the capacitor so that the start switch and capacitor were integral, and so keep the overall length of capacitor and switch as short as possible. The output of the start switch had to be through a cable of fixed diameter to the existing load assembly. These requirements together with the maximum switch diameter mentioned earlier, and the ever present urgency associated with project work limited our freedom of design. Reduction of 'jitter' (overall spread in the firing times of a switch) with a reduction in inductance looked feasible with electrode configurations similar to those of Westendorp[3,4], particularly if the intermediate electrode potential was violently altered on triggering. The principle is shown in Fig.2. The thin centre electrode is made coincident with an equipotential line between the main electrodes under d.c. conditions. On displacing the potential of this electrode, which occurs when the spark gap is triggered, severe electrical stressing results along its edges leading to rapid electrical breakdown of the main gap.

In the prototype design the 40% equipotential line (0.4 V) was chosen so that when a trigger pulse of -2 V was applied then the uniform field stress in the gaps on both sides of the trigger electrode would be the same. The final electrode configurations are different in detail and will be described later. We have called this type of switch a 'field distortion' switch.

Throughout the testing of all these switches compressed air has been used to pressurise them, dried to a dew point of better than -30°C (0.3 g/m^3).

3. START SWITCHES

3.1 Design

In reducing the inductance of the original capacitor/start switch assembly the junction terminations had to be redesigned. Fig.3(a) shows the original

1. INTRODUCTION

A shock heated plasma experiment called Tarantula[1] required a current discharge of 1.2 MA rising in 1 μsec from a 100 kV source with an initial rate of current rise 2.5×10^{12} amps/sec. Forty 0.5 μF 100 kV capacitors were individually connected to start-switches of the triggered spark gap type described in 1962[2] and then by separate lengths of cable to a low inductance discharge tube. These start switches have been used successfully since then. However, to obtain a greater rate of rise of current an even lower inductance system would be desirable for future experiments. Analysis of the Tarantula circuit elements showed that the discharge tube inductance could be reduced by subdivision into shorter sections, but it would then be essential to reduce the inductances of the capacitors, switches and cable. Although it has proved just possible to develop a lower inductance cable (70 nH/m as against 125 nH/m) it would still be desirable to reduce the length of each cable from 1.8 m to 0.9 m. This would bring the switches electrically closer together and mounting the switches in a circle as on Tarantula would mean that the overall diameter of the switches could not exceed 25 cm. Furthermore, the spread in the firing times of the first to last switch would have to be half that of the Tarantula switches to avoid the early firing of one switch upsetting the firing of the later ones.

Such a start switch has now been developed, and in the course of the investigations it was found that with small modifications the usefulness of this type of switch could be extended to carry out two further switching functions. One of these is to produce a half sine wave of current (with a frequency of 250 kc/s) by short circuiting the source capacitor and start switch at first current zero. This process is known as 'diverting'. The other function is to produce a long current pulse by short circuiting the inductive load at current maximum. This process is known as 'clamping' or 'crowbarring'. The current and voltage waveforms which result from these switching functions are shown in Fig.1. This paper describes the switches which have been developed for the three switching functions 'starting', 'diverting' and 'clamping'.

2. PRINCIPLES OF DESIGN

The Tarantula start switches had to be designed to plug into the re-entrant termination of a capacitor whose design had already been frozen. Due to the long time required for developments on capacitors only minor modifications which gave rise to a large benefit could be considered. It was therefore decided to alter only the output termination of the capacitor so that the start switch and capacitor were integral, and so keep the overall length of capacitor and switch as short as possible. The output of the start switch had to be through a cable of fixed diameter to the existing load assembly. These requirements together with the maximum switch diameter mentioned earlier, and the ever present urgency associated with project work limited our freedom of design. Reduction of 'jitter' (overall spread in the firing times of a switch) with a reduction in inductance looked feasible with electrode configurations similar to those of Westendorp[3,4], particularly if the intermediate electrode potential was violently altered on triggering. The principle is shown in Fig.2. The thin centre electrode is made coincident with an equipotential line between the main electrodes under d.c. conditions. On displacing the potential of this electrode, which occurs when the spark gap is triggered, severe electrical stressing results along its edges leading to rapid electrical breakdown of the main gap.

In the prototype design the 40% equipotential line (0.4 V) was chosen so that when a trigger pulse of -2 V was applied then the uniform field stress in the gaps on both sides of the trigger electrode would be the same. The final electrode configurations are different in detail and will be described later. We have called this type of switch a 'field distortion' switch.

Throughout the testing of all these switches compressed air has been used to pressurise them, dried to a dew point of better than $-30^{o}C$ ($0.3\ g/m^3$).

3. START SWITCHES

3.1 Design

In reducing the inductance of the original capacitor/start switch assembly the junction terminations had to be redesigned. Fig.3(a) shows the original arrangement and Fig.3(b) the final design of the capacitor termination. The major differences are:-

(1) As the capacitor termination forms part of the switch the material chosen for this was electrical grade porcelain instead of epoxy resin which had been used previously. (This means that arc deposits can be removed from the surface and damage from surface flashovers is not serious.)

(2) The capacitor termination must be pressure tight to withstand up to 100 p.s.i.g. of compressed air (this controls the allowable shape of the porcelain) and the profile of the porcelain must be such as to keep the electric stress as low as possible.

(3) The centre metal connector of the capacitor is made larger in diameter to allow a lower inductance connection to be made.

For the switch two basic geometries were considered, the first plane parallel and the second coaxial, called type C and type D respectively, following the type B used on the actual Tarantula experiment. Both these switches have cable output terminations. For another experiment (a cusp injection experiment called CUSIE) a transmission line output was needed and for this the type C switch was modified. All three variants and the original type B switch are shown in Fig.4.

We investigated both geometries as, although their inductances were similar, their operating characteristics might have been different. For example

(1) Plane parallel geometry might be less liable to spurious firing.

(2) Triggering with cylindrical geometry might be more effective.

(3) The insulating surfaces in cylindrical geometry are shielded from the arc channel by metal electrodes.

(4) Manufacture might prove easier or more economical in one form than in the other.

The electrode spacing was determined by compromising between a small spacing with high air pressure which would improve the flashover of the insulating surfaces and give a wider voltage operating range, and a large spacing with lower air pressure which would make manufacture easier by relaxing tolerances, an important consideration in making tens or hundreds of identical units. It was also felt that the smaller the main gap the thinner the centre electrode would have to be to prevent over-stressing. The main gap finally chosen was 10 mm and the thickness of the centre electrode 0.8 mm.

In the first tests the intermediate electrodes were sharpened to a knife edge in the belief that this would distort the pre-trigger field less than a rounded edge, and that on triggering the field at the sharp edge would be extremely high, giving rise to field emission and to a shorter and less 'jittery' breakdown. However it was found that the knife edge quickly became burnt and distorted. A plain disc 0.8 mm thick with a rounded edge was substituted and after firing it was found that the burning on the edge was negligible and the performance of the switch unchanged.

Using the cable output connection shown in Fig.4 (a),(b) or (c), the inductance of the termination was considerably reduced from that of the type B switch. The liquid grading was eliminated and the electric stress along the insulating tube and cable insulating surfaces controlled electrostatically by careful shaping. No trouble with this termination has been experienced up to 100 kV as long as the joint is well made and cable surface is well greased with petroleum jelly. The insulating tube is remote from the arc discharge and arc products.

The ringing frequency of the 0.5 μF capacitor on short circuit was 625 kc/s. With a short circuit just outside the switch this frequency fell to 550 kc/s. The inductance of the capacitor was therefore 130 nH and the added inductance of the switch was 35 nH. The inductance of the type B capacitor/switch combination on Tarantula was 340 nH.

3.2 Tests

The test circuit shown in Fig.5 was set up to investigate the characteristics of the start switches. The d.c. potential on the trigger electrode is controlled by the potentiometer (X) and the d.c. potential of the trigger cable is controlled by (Y). The trigger pulse is applied by closing the solenoid operated switch (Z) which sends a reverse polarity pulse up the cable to the spark gap where it doubles and passes through the blocking capacitor onto the intermediate electrode.

The blocking capacitor lets the fast trigger pulse through (~ 10 Mc/s) but prevents too much current loss from the main discharge circuit, normally at a frequency of 100 - 250 kc/s.

The first tests were made to ascertain the accuracy with which the voltage on the intermediate electrode had to be set. This voltage was varied between 36% and 44% of the total voltage across the gap for an electrode which was placed at the position which the 40% equipotential would normally lie, and the static breakdown values of the switch were determined for various switch pressures up to 60 kV (Fig.6). Above 70 kV at the reduced pressure necessary for this test, there was a tendency for the porcelain bushing of the capacitor to flash-over before the main gap. The breakdown value changed by only 10% for the 36 - 44% variation and the value obtained for the 40% setting was what would be expected for a uniform field gap reduced by the thickness of the centre electrode. The voltage setting on the intermediate electrode was not therefore critical and all further tests were carried out with the nominal 40% value.

The trigger pulse rise time was first adjusted to be equal to that produced by a master switch with 40 cables as on the Tarantula experiment. A few further tests were also made with both longer and shorter rise times giving slightly different results. Some variation in the absolute values of the breakdown results are probably due to unintentional variation in the rise time of the trigger pulse. The signals which arrive at the start switch are shown in Fig.7(a) and when breakdown occurs these are modified as shown in Figs.7(b) and 7(c). The distorted field for different voltages on the trigger electrode is shown in Fig.8, the definition being made that for a capacitor voltage of, say, + 100 kV, a 50% trigger means that the trigger cable was charged to + 50 kV. On short circuiting the end of the trigger cable, a - 50 kV pulse passes down the trigger cable and doubles in value on reaching the high impedance of the switch, driving the intermediate electrode to 40 - 100 = - 60 kV. Outlines of the edge of the trigger electrode as manufactured and after being in operation for thousands of discharges are shown in Fig.9.

The trigger voltage into the start switch was measured with a cable capacitance divider and the output from the start switch was measured either by another capacitance divider or by a pick-up coil near the load circuit. The breakdown time of the gap is defined as the time (T) measured from oscilloscope waveform photographs and a typical measurement is shown in Fig.7. The majority of tests were made with oscilloscopes which had a rise time of 12 nsec and so the real rise times of the pulses were shorter than normally recorded. A few tests were made with an oscilloscope with a rise time of 0.32 nsec.

The range of variables which could be justifiably investigated are considerable. They are:-

(i)	Voltage across gap	0 - 100 kV
(ii)	Voltage of trigger circuit	0 - 100 kV
(iii)	Pressure inside gap	0 - 100 psig
(iv)	Ringing frequency of main circuit	70 - 500 kc/s
(v)	Rise time of trigger pulse	1 - 30 nsec
(vi)	Permutations on polarity of main and trigger potentials	
(vii)	Spacings between electrodes.	

In practice restrictions had to be imposed and so the test conditions were selected which would give the operating characteristics of the switches without examining all the possibilities. For example, when checking freedom from flashover we used the lower ringing frequencies of the main circuit (~ 100 kc/s) so that the maximum voltages were applied to the electrodes. When examining electrode erosion with high currents we operated at the maximum ringing frequency (~ 500 kc/s) to increase the coulomb flow. Furthermore, the insulation level was marginal at 100 kV with the maximum design operating pressure of 100 psig and therefore the data for this condition is small. Minor design changes for a production model would remove this difficulty which is mainly associated with the centre electrode bushing. Breakdown tests were not affected by the main operating frequency, and the bulk of the tests were at about 80 kc/s.

The results are recorded in Figs.10 and 11 for a positively charged capacitor and trigger cable and measurement of 'jitter' for the same conditions are shown in

Figs.12 and 13. When the trigger cable was charged negatively with the discharge capacitor still charged positive the behaviour of the switch was quite unpredictable. When both the trigger cable and the discharge capacitor were charged negatively, the switch would fire over a fairly wide range of voltage and pressure. However, under this condition, the breakdown times were very variable and seemed to be only weakly dependent on pressure, Fig.14. Fig.15 shows the effect on the jitter measurement of increasing the rise time of the trigger pulses to 30 nsec. A few tests were done with the overall gap spacing 7.5 mm instead of 10 mm, keeping the central electrode at 40% of the new spacing. The breakdown times decreased in proportion to the spacing, that is by 25%. On raising the pressure so that the 'pressure × spacing' product was the same as previously the same breakdown times were obtained.

A detailed analysis of the breakdown mechanism is given in section 6.

During the course of this work there were many thousands of discharges through the switches at various currents up to 75 kA with a charge flow of 0.5 coulombs per discharge. The characteristics of the switches were unchanged at the end of the tests, apart from the drift with exceptionally long trigger rise times as shown in Fig.15, and the damage to the electrodes was comparatively slight. By placing a short circuit just outside the switch a current of 120 kA at 550 kc/s was produced. After 20 discharges the electrodes were examined and no difference in the erosion could be seen between these discharges and the previous ones. The current limitation of the switches under these conditions must therefore be considerably above 120 kA.

4. DIVERT SWITCH

4.1 Design

Examination of the appropriate waveforms in Fig.1 shows that the divert switch has to be able to withstand the rapidly changing voltage across it (frequency 250 kc/s for the CUSIE experiment) and yet fire precisely when triggered. The overall system jitter for this switching function had to be less than 30 nsec which meant that the spark gap itself had to be better than ± 10 nsec. Furthermore the voltage across the switch at the time of firing would be negative and only 80 - 90% of the initial value half a cycle earlier. For the CUSIE experiment this switch required connection to parallel plate transmission lines and the diverted current per switch with an initial capacitor voltage of 60 kV would be 75kA.

One of the principal difficulties with this switch was to keep the intermediate electrode at its correct proportion of the rapidly varying voltage across the gap. Inductive dividers using external cables, or capacitive dividers can be used, but we chose to make a low inductance resistive divider using a thin cylinder of electrolyte as shown in Fig.16. This resistor is a key part of this switch. The inductance of the resistor was 7 nH per half which was adequately low. The lower the resistance value the more exactly would the oscillatory voltage be followed. However with too low a resistance the trigger voltage applied to the intermediate electrode would be short circuited. Calculation showed that an overall resistance of 500 ohms would be a reasonable compromise. The trigger voltage appearing on the trigger electrode for varying resistances of the divider is shown in Fig.17.

When the trigger cable is connected to the intermediate electrode it throws a capacitance of 200pF onto the earthy half of the gap which unbalances the potential division of a rapidly varying voltage. The effect of the unbalance can be removed by increasing the operating pressure but this limits the maximum voltage at which the gap will operate to 60 kV at 80 psig; at 70 kV even 110 psig will not suffice to prevent premature firing. In addition the operating pressure range is limited to about ± 5 psig. However by inserting a spark gap in the circuit as in Fig.19 the trigger circuit can be isolated from the intermediate electrode until the trigger pulse is applied when the isolating gap is over-volted by a factor of three and under these conditions the operating pressure range is very much larger.

It is important that the divert switch should have as low an inductance as possible if the current in the load after diversion is to be kept to a minimum.

The current waveform achieved in practice is shown in Fig.19(b) instead of the ideal waveform in Fig.19(a). The residual oscillatory current (R) depends on the divert switch inductance and the inductance back to and including the capacitor, assuming the load inductance is much greater than the switch inductance. For the design of Fig.16 the divert switch inductance was 55 nH, the inductance on the capacitor side was 140 nH and the load 840 nH. If the divert switch is not fired at the correct time there is a d.c. component (S) which dies away exponentially and Fig.19(c) shows the effect of firing early.

4.2 Tests

Two different conditions were tried, the test circuit diagram being shown in Fig.18. Test voltages were from 20 - 70 kV, the top limit being determined by flashover of the transmission lines. The divert switch was triggered by a low inductance trigger switch which was fired by a 15 kV hydrogen thyratron. The pulse to fire the thyratron was derived from a pick up coil near the load inductance which sensed the initial voltage pulse of the discharge and operated a variable delay unit which in turn triggered the thyratron. The load circuit was adjusted until the operating frequency was 230 kc/s and the negative peak voltage about 90% of the initial position voltage. Jitter in the test trigger system (including the delay element) was ± 25 nsec, and so as long as the jitter of the switch was not greater than ± 5 nsec the overall jitter would be within the ± 30 nsec requirement mentioned earlier.

As the main circuit frequency was 230 kc/s the optimum delay before firing the divert switch was 2.2 μsec. Test results given in Table A show the effects of different delay times, the trigger voltages used being either 45 or 50 kV. By varying the distribution of inductance in the circuit, the voltage on the divert switch was varied from 65 - 90% of the capacitor voltage, and therefore allowing for the 90% reversal the divert switch fired at 60 - 80% respectively of the capacitor voltages. The results quoted are the actual voltages first applied to the divert switch; the divert switch will have fired at 90% of these. The tests were made to establish the maximum pressure at which the switch will fire without exceeding the 5% d.c. component limit due to late or early firing. The lowest operating pressure will be that at which the switch does not fire prematurely. The results are given in Table A and the operating range is shown in Fig.20, the polarity of the trigger appears to be unimportant.

5. CLAMP SWITCH

When investigating the operating range of the start switches we found that even pressurised to 90 psig they could be fired with a capacitor voltage of only 170 volts as long as a high trigger voltage (~ 50 kV) was used. No breakdown or jitter measurements were made but it did seem that we might be able to use this design as a clamping switch, which is required to hold off full circuit volts and yet fire with near zero voltage across it. Accordingly we tested the divert switch as a clamp switch by merely changing the time at which the trigger pulse was applied.

Initially it was decided to try clamping for two different rise times of the main current discharge, 1.1 μsec and 3 μsec corresponding to a discharge frequency of 230 kc/s and 80 kc/s which gave currents in the load circuit of 40 kA and 15 kA respectively, when the main ½ μF capacitor was charged to 60 kV. The initial voltages which appeared across the clamp switch under these conditions were 54 kV and 59 kV. Additional tests on a larger capacitor bank were made to determine the coulomb rating at 100 - 200 kA with a rise time for the main discharge current of 8 μsec, frequency 30 kc/s. The initial circuits used are shown in Fig.18. The resistances of the clamp switch are mainly due to the arc drop which is about 60 volts and the charge flow per discharge is 2 coulombs. Typical waveforms are given in Fig.21 where it can be seen that the ripple on the clamped current is less than 5% of the initial current and rapidly dies away.

Summarising the results for this switch we found that with the clamp triggering at the optimum time the current could be clamped at 90 - 100% of its peak unclamped value, the firing time of the clamp switch being ~ 100 nsec. 90 - 95% of the peak unclamped current could be obtained even when firing 200 nsec earlier (or later) than the optimum time even with a main current discharge which rose in 1.1 μsec. Some thousands of discharges were fired at about 2 coulombs at a variety of conditions the switch behaving satisfactorily and its performance was unchanged from the beginning to the end of the tests. At a higher coulomb rating the switch again behaved satisfactorily without undue wear at 100 - 200 kA and 20 coulombs using brass electrodes and this could certainly be increased by using more arc resistant materials. It was noticeable that at 100 kA and above the main arc of the discharge occurred away from the edge of the trigger electrode so that erosion of this electrode was not excessive.

Comparison of this clamp switch with available ignitrons for clamping duty shows:

(1) Ignitrons do not operate reliably above 20 kV. The field distortion clamp switch has operated at over 60 kV and should be capable of 100 kV with modification to the transmission line. This type of clamping switch could be designed to work at higher voltages.

(2) Ignitrons can not be operated at frequencies as high as 250 kc/s because their triggering times are too long.

(3) Current reversal in the switch due to oscillations from the capacitor bank is unimportant with this switch although it is serious in ignitrons without special metal anodes.

(4) The maximum peak current that an ignitron will carry is usually 100 kA. This switch has carried 200 kA and could probably carry considerably more.

(5) The charge flow which can be successfully carried by this switch for a reasonable life is 20 coulombs. A small ignitron will carry about 10 coulombs and a large ignitron will carry 400 coulombs.

(6) The inductance of a large ignitron (20 kV) will be about 500 nH, a small 20 kV ignitron about 40 nH. This switch has an inductance of 50 nH for 60 - 100 kV.

(7) The arc drop in the switch is about 60 volts and in an ignitron will be of the order of 100 volts for times $<$ 100 μsec.

(8) Ignitrons fire only when the anode is positive with respect to the cathode. For this switch polarity does not matter.

6. MECHANISM OF BREAKDOWN

Due to the intention to use the original Tarantula Master Switch all the initial work on the start switches was done with a trigger voltage rise time of about 10 nsec and later the trigger rise times of 1, 10 and 30 nsec were investigated. As the trigger cable length was about 50 nsec (8 m with a voltage propagation of 6 nsec/m) the 30 nsec rise time pulse was distorted as shown in Fig.22. The other shorter rise time pulses were not distorted and both actual measurements and the analogue computer runs indicated that the waveforms entering the switch were faithfully reproduced at the trigger electrode after passing through the circuit of the trigger system which is also shown in Fig.22.

Breakdown time results comparing these three rise times of the trigger pulses are shown in Fig.22 and three features can be seen:

(i) The minimum trigger voltage (20 - 25%) which will produce breakdown is the same for the three rise times.

(ii) The longer rise times lead generally to a longer breakdown time, but these times become equal at about 150% trigger.

(iii) Above 150% the breakdown times reach a constant value no matter how high the trigger voltage is.

As the amplitudes for the trigger waveforms are the same the first feature is to be expected. That longer rise times lead to a longer breakdown time is also to be expected and examination of Fig.24 shows why the 30 nsec rise time eventually becomes equivalent to the 10 nsec rise time at about 150% trigger. That illustration shows the 30 nsec rise time pulse expanded by a factor of two and three. Assuming that this is the change from 50% to 150% trigger it becomes apparent that identical breakdown times will be obtained as breakdown under these conditions is occurring on the leading edge of the pulse.

From the trigger waveforms in Fig.7 with and without breakdown it can be seen that the first 'breakaway' at point (A) corresponds to breakdown between the trigger electrode and the capacitor electrode, the remaining part of the breakdown time will be that of the trigger and capacitor electrodes to the load electrode.

If this is so then the second stage breakdown time will be constant for constant capacitor voltage and pressure and will not be dependent on the trigger voltage or its waveform. The results are given in Fig.25 and confirm this, showing that overall breakdown is a 'cascade' mechanism. What is not so predictable is the asymptotic approach to a fixed breakdown time for the first stage irrespective of the trigger voltage. It is suggested that corona may limit the stress which would otherwise occur.

To keep the static breakdown voltage equal to that which would be expected from plain parallel electrodes, it would be thought that the intermediate electrode should taper very slowly to a knife edge. Furthermore the knife edge should assist triggering as any displacement of its potential should result in infinite stress at its edge. However as described earlier a rounded electrode performed just as well, and it is particularly noticeable that after a number of discharges had been fired and the electrode distorted as shown in Fig.9 nevertheless the discharges were taking place at random around the circumference so that the trigger electrode was uniformly eroded.

Using a digital computer the equipotentials between the electrodes were plotted for both the untriggered and the triggered conditions. Some of these are shown in Fig.8. From these the stresses were determined and plotted in Fig. 26. Under static conditions, although the stress at the edge of the intermediate electrode was above the uniform field breakdown value, no corona could be detected (< 1 μA) right up to the static breakdown values. Corona inception was therefore measured with the intermediate electrode at different potentials and the capacitor and load electrodes at zero potential. The results of this test are plotted in Fig.27 together with the edge stresses obtained from the computer plots. For interest Peek's formula[5] is plotted with the 'wire' radius equal to the nominal radius of curvature of the edge of the intermediate electrode. Although Peek's formula is proved only for pressures below and up to atmospheric pressure, and the plot extrapolates his formula to 4 atmospheres gauge the agreement is quite good. We do not know of any other experimental data in this region where the corona stress has been determined.

Measurements were made of the conditions both untriggered and triggered under which the switches did just fail to breakdown. The results are given in Table B which shows the various stresses calculated. Although the edge stress is 1.45 times the greater of the two uniform field stresses in the untriggered cases breakdown appears due to the normal uniform field criterion. In the triggered cases the uniform field produced is lower than the breakdown value and the edge stresses, which are from 2.2 (at 20% trigger) to 2.85 (at 50% trigger) times greater than the uniform field values, must have an effect. From the equipotentials the field around the edge becomes equal to the uniform field at about one radius from the edge (0.4 mm) for the untriggered condition and at four radii from the edge (1.6 mm) in the triggered conditions. This greater extension of the high field must have an important effect on the breakdown. It can also be seen from the table that corona was not detected under static conditions as the edge stresses are well below the corona inception stresses. For the triggered state the edge stresses are in the region of the corona inception stresses.

If the trigger voltage is gradually increased whilst maintaining all the other conditions constant, the breakdown time first decreases and then remains constant. Table C shows the values at which the constant region is first approached. It will be seen that the uniform region exceeds the uniform field breakdown by factors which vary from 4 (at a capacitor voltage of 10 kV) to 1 (at a capacitor voltage of 100 kV). Over the same range the ratio of the edge stress to the corona stress varies from 8 to 2, and the ratio of edge stress to the uniform field breakdown stress varies from 24 to 2.5.

It has already been shown that this type of switch breaks down in the 'swinging cascade' mode which was also the mode of the Tarantula type B switch. Fig.28 shows however, that for the same conditions of electrode spacings, pressure, charging voltage, trigger voltage and trigger rise time the present design has a breakdown time of 45 nsec compared with a breakdown time of 70 nsec for the type B switch. It should be noticed that the Tarantula type B switch is a swinging cascade spark gap with an auxiliary fourth electrode to provide illumination of the two main gaps. The field distortion switches are not provided with a similar illuminating gap.

This faster breakdown of the field distortion switches must be due solely to the higher fields produced by the field distortion method and with the faster breakdown times goes the lower jitter.

7. CONCLUSIONS

The switch described is of low inductance (55 nH), and the prototypes tested will operate up to 100 kV and will carry out the functions of starting, diverting and clamping with currents of 200 kA and a charge flow per discharge of at least 5 coulombs. The jitter of the breakdown time is about ± 5 nsec. The life under these conditions is expected to be several thousands of discharges. The switches are insensitive to changes in internal air pressure and trigger voltage over wide ranges. Eight have been used satisfactorily in parallel on one experiment with transmission line output such that the time for signals to pass from the output of one gap to another was 10 nsec.

It is believed that this type of switch could be designed to do the three functions of starting, diverting and clamping at voltages in excess of 100 kV and coulomb flow in excess of 20 coulombs.

8. ACKNOWLEDGEMENTS

We wish to thank D. Bold, C.E. Brookes, J. Reid, P.H. Thearle and A.J. Whyte who assisted with the design and carried out the experimental work. We would also like to thank G. Bate who produced the digital computer programme which enabled the equipotential plots to be made and to K. Sinton who made the various analogue computer runs.

British Insulated Callender's Cables Ltd. at Helsby and at Belvedere developed the 100 kV capacitors and cables.

9. REFERENCES

1. BELL, W.R. and others. Tarantula - a 100 kV pinch discharge apparatus for studying shock waves. (In course of publication).

2. BISHOP, A.E., EDMONDS, G.D. and SHEFFIELD, J.S. A 100 kV switch for rapid discharge of high energy capacitors. J. Sci. Instrum., 1962, 39, p.566.

3. WESTENDORP, W.F. Switching of high currents in fast and slow plasma compression systems. 1961, G.E. Research Lab. report 61-RL-2662E.

4. GOLDMAN, L.M., POLLOCK, N.C., REYNOLDS, J.A. and WESTENDORP, W.F. Spark-gap switching of a 384 kJ low inductance capacitor switch. Rev. Sci. Instrum. 1962, 33, p.1041.

5. PEEK, F.W. Dielectric phenomena in high voltage engineering, 3rd ed. New York, McGraw Hill, 1929.

TABLE A

DIVERT SWITCH TEST RESULTS

All these tests were made with a main discharge frequency of 230 kc/s (2.2 μsec half period). Variation of d.c. component is the sum of the jitters of the divert trigger delay box, divert thyratron and divert master switch.

Capacitor Charging (kV)	Trigger Cable Charging (kV)	Air Pressure (psig)	Delay of Trigger from t = 0 (μsec)	% d.c. Component	
				Mean	Spread
+ 20	- 45	0	2.5	+ 15	+ 5 - 5
		10	2.5	+ 17	+ 6 - 7
		20	2.5 failed to divert		
		10	2.15	- 1	+ 29 - 10
		10	2.0	- 26	+ 9 - 17
+ 40	- 45	0	2.15	+ 18	+ 21 - 1
		10	2.15	- 10	+ 2 - 1
		20	2.15	- 8	+ 3 - 1
		20	2.2	+ 1	+ 5 - 3
		20	2.05	- 24	+ 3 - 3
		30	2.15	- 9	+ 4 - 2
		40	2.15	- 9	+ 4 - 6
		50	2.15	- 4	+ 29 - 7
		60	2.15 failed to divert		
+ 60	+ 50	70		- 5	+ 10 - 3
+ 70	+ 50	90		+ 2	+ 6 - 10
+ 70	- 50	90		+ 5	+ 3 - 20
+ 60	- 45	10	fired spuriously		
		20	2.2	0	
		30	2.2	0	
		40	2.2	+ 3	+ 7 - 3
		40	2.52	+ 30	+ 5 - 5
		40	2.04	- 20	+ 5 - 5
		50	2.2	+ 10	+ 32 - 10
		60	2.2	+ 7	+ 30 - 9
		70	2.2	+ 16	+ 19 - 14

TABLE B

ELECTRICAL STRESS VALUES WHEN THE SWITCHES ARE JUST FIRING

(triggered and untriggered)

Capacitor Charging Voltage kV	Trigger Voltage % of Capacitor Voltage	Air Pressure p.s.i.g.	Uniform Field Stress Capacitor side / Load side kV/cm	Uniform field Breakdown stress kV/cm	Stress at edge of Intermediate Electrode kV/cm	Corona Inception Stress Positive/Negative kV/cm	Type of Spark Gap	Ratio of edge Stress to max. Uniform Field Stress
20	0	- 3	22/22	24	32	75/79	C	1.45
	0	- 3	22/22	24	32	75/79	D	1.45
	25	0	40/6	30	94	86/86	D	2.35
	50	20	58/34	70	166	160/137	C	2.85
40	0	5	44/44	40	64	105/98	C	1.45
	0	10	44/44	50	64	123/112	D	1.45
	25	30	80/12	92	188	198/163	C	2.35
	25	30	80/12	92	188	198/163	D	2.35
70	0	20	77/77	70	110	160/138	C	1.45
	0	25	77/77	80	110	180/150	D	1.45
	25	80	140/21	192	330	386/292	D	2.35
	35	80	161/63	192	420	386/292	C	2.6
90	0	30	99/99	92	144	198/163	C	1.45
	20	95	163/0	223	360	445/330	D	2.2
	25	95	180/27	223	423	445/330	D	2.35
	35	100	207/81	235	540	463/343	C	2.6
100	0	35	110/110	100	166	217/176	C	1.45

TABLE C

ELECTRICAL STRESS VALUES FOR BREAKDOWN TIMES INDEPENDENT OF TRIGGER VOLTAGE INCREASE

Capacitor Charging	Trigger Voltage % of Cap	Air Pressure (psig)	Uniform Field Stress cap / load Electrode kV/cm	Uniform Field Breakdown Stress kV/cm	Stress at edge of Intermediate Electrode kV/cm	Corona Inception Stress pos / neg kV/cm	Type of Spark Gap	Breakdown time (nsec)	Ratio of Uniform Stress to B/d stress	Ratio Edge Stress/Corona Stress	Ratio of Edge Stress to Uniform Field B/d Stress
10	350	0	120/185	30	705	86/86	C	78	4.0	8.3	23.5
20	100	0	94/94	30	340	86/86	D	70	3.1	3.95	11.3
20	200	20	130/150	70	560	160/137	C	88	2.15	4.1	8.0
20	250	10	195/260	50	1000	123/112	C	78	5.2	8.1	20.0
40	75	30	150/126	92	500	198/163	CUSIE	60	1.63	3.07	5.4
40	75	30	150/126	92	500	198/63	D	55	1.63	3.07	5.4
40	50	10	120/68	50	330	123/112	D	40	2.4	2.95	6.6
50	90	50	210/200	130	760	273/226	C	62	1.6	3.3	5.8
50	70	40	180/140	110	580	235/190	C	54	1.6	3.0	5.3
70	70	70	250/200	170	810	348/286	C	54	1.47	2.83	4.8
70	75	80	260/220	192	870	386/292	D	50	1.35	3.0	4.5
70	50	40	200/120	110	580	235/190	D	46	1.8	3.05	5.3
90	50	95	260/150	223	750	445/330	D	51	1.17	2.27	3.36
90	50	110	260/150	255	750	300/400	D	53	1.0	2.0	2.95
100	50	110	290/170	255	830	500/400	D	50	1.0	2.0	3.25

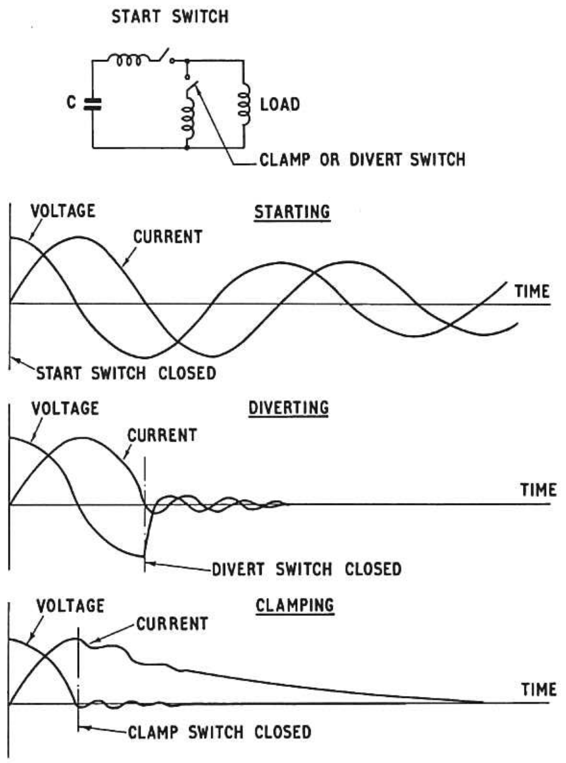

Fig.1 (CLM-P81)
Current and voltage waveforms for the switching functions 'Starting' 'Diverting' and 'Clamping'

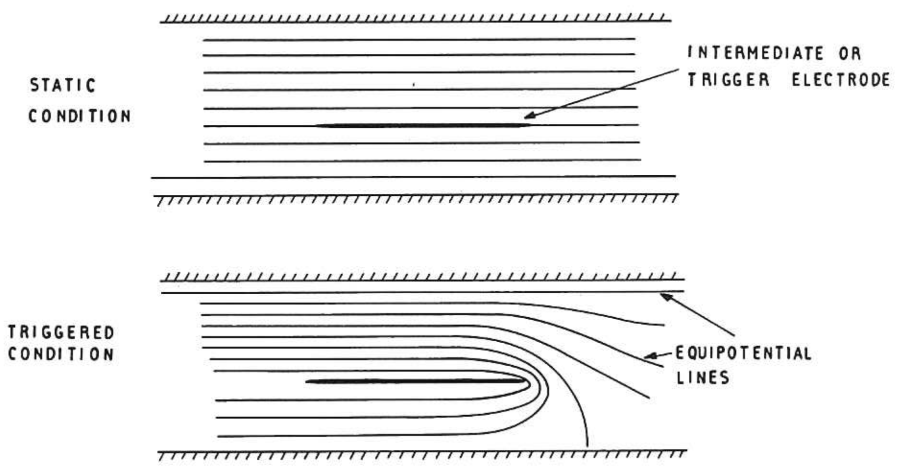

Fig.2 Principle of the field distortion switch (CLM-P81)

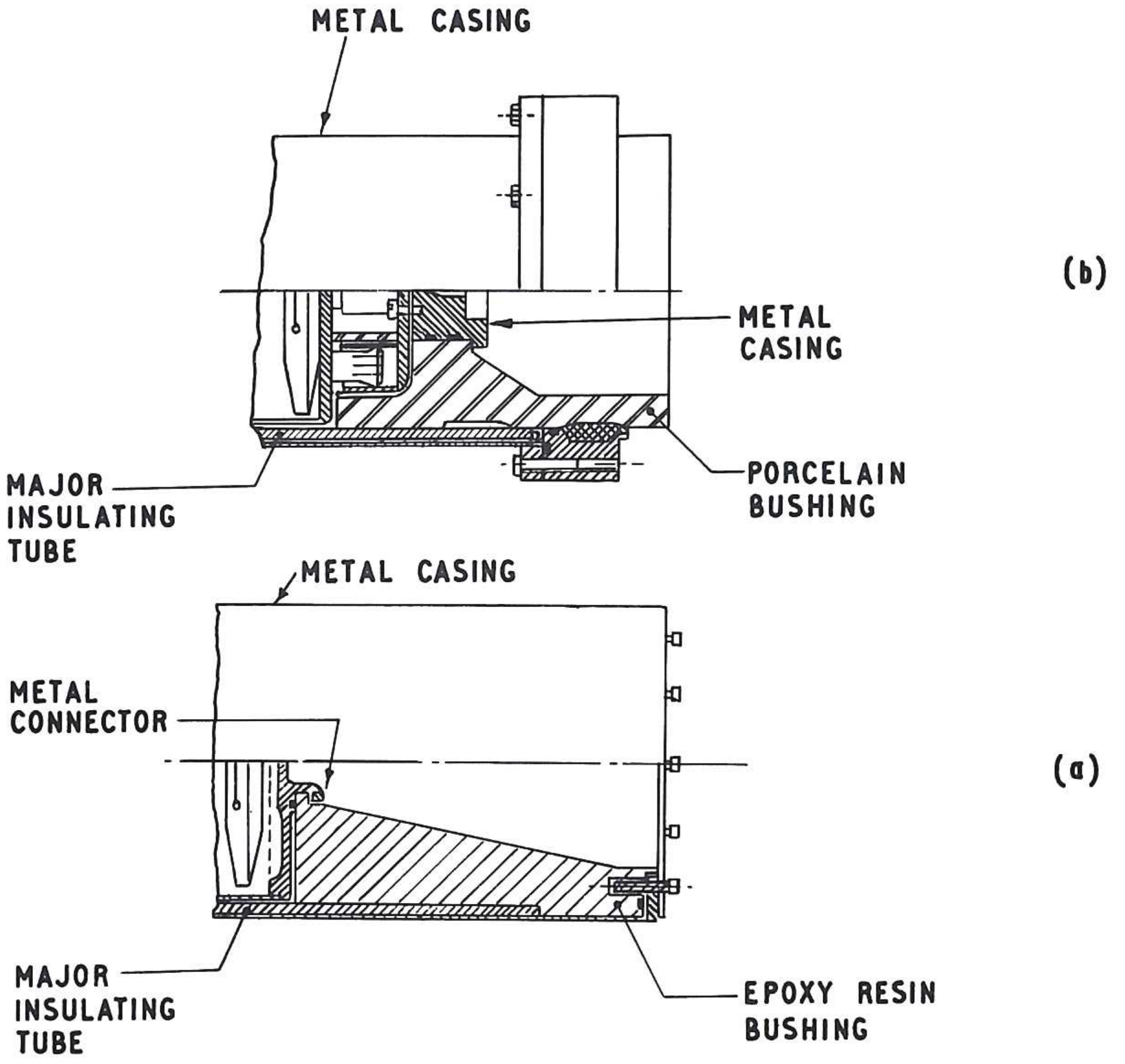

Fig.3 Capacitor terminations (CLM-P81)

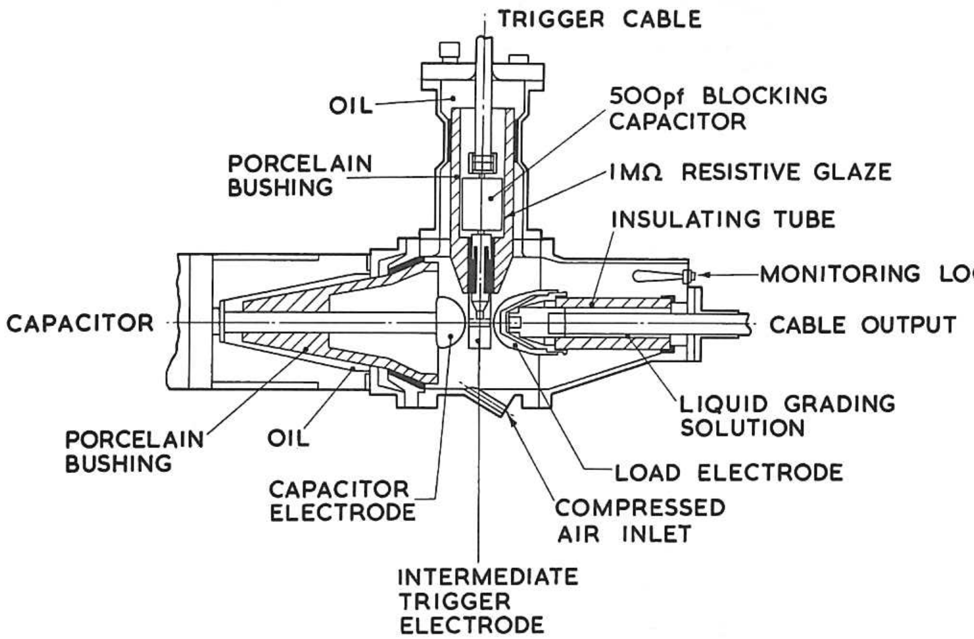

Fig.4(a) Start Switch Type B (CLM-P81)

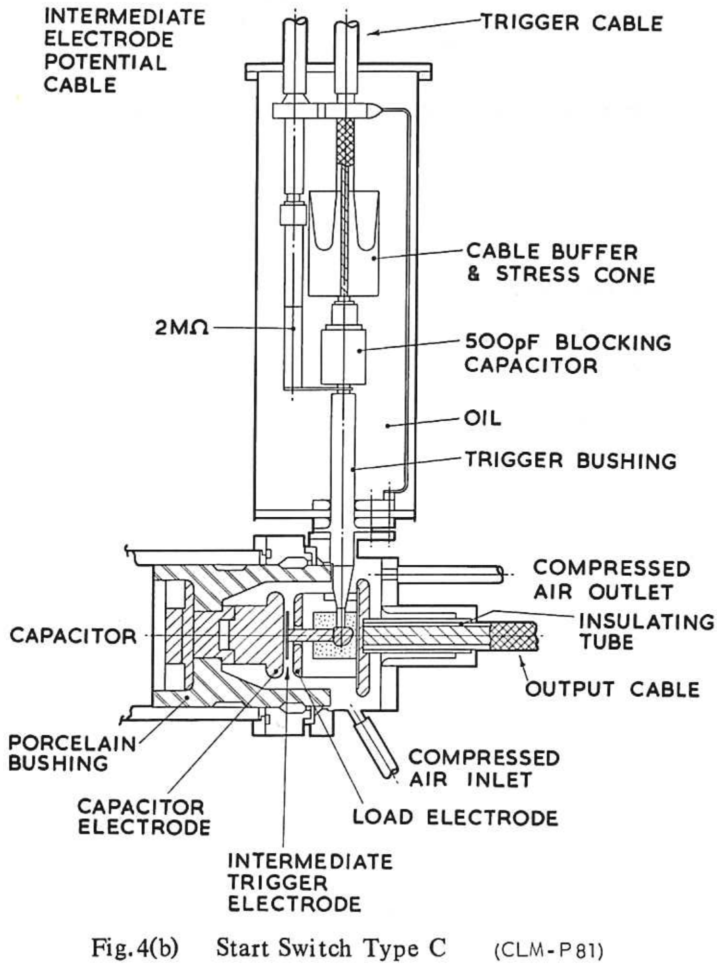

Fig.4(b) Start Switch Type C (CLM-P81)

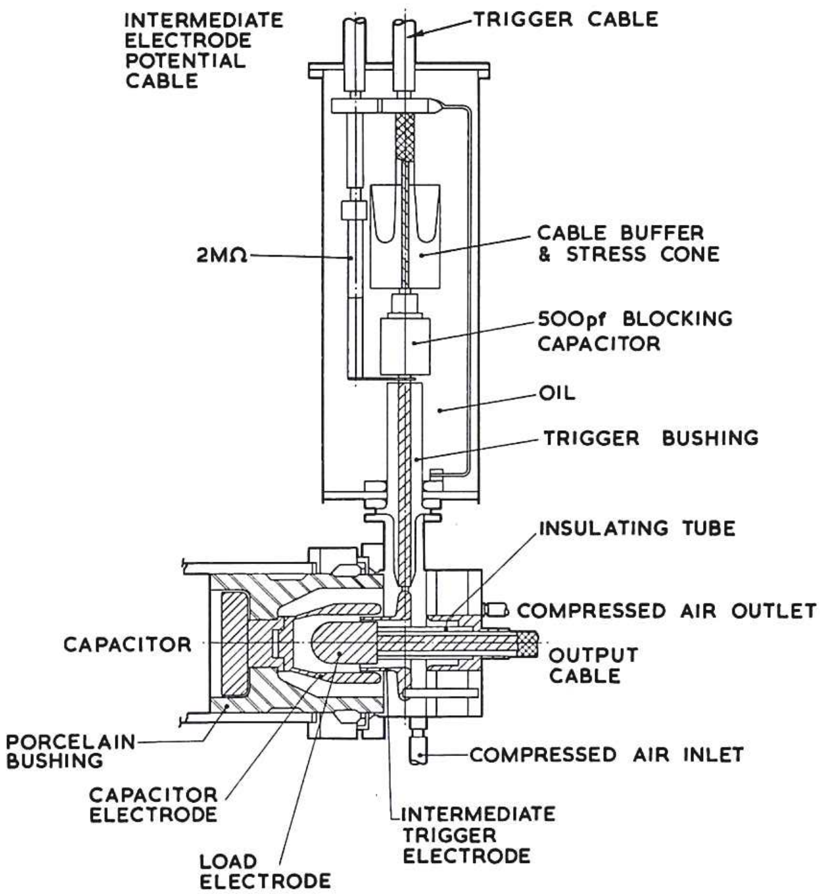

Fig.4(c) Start Switch Type D (CLM-P81)

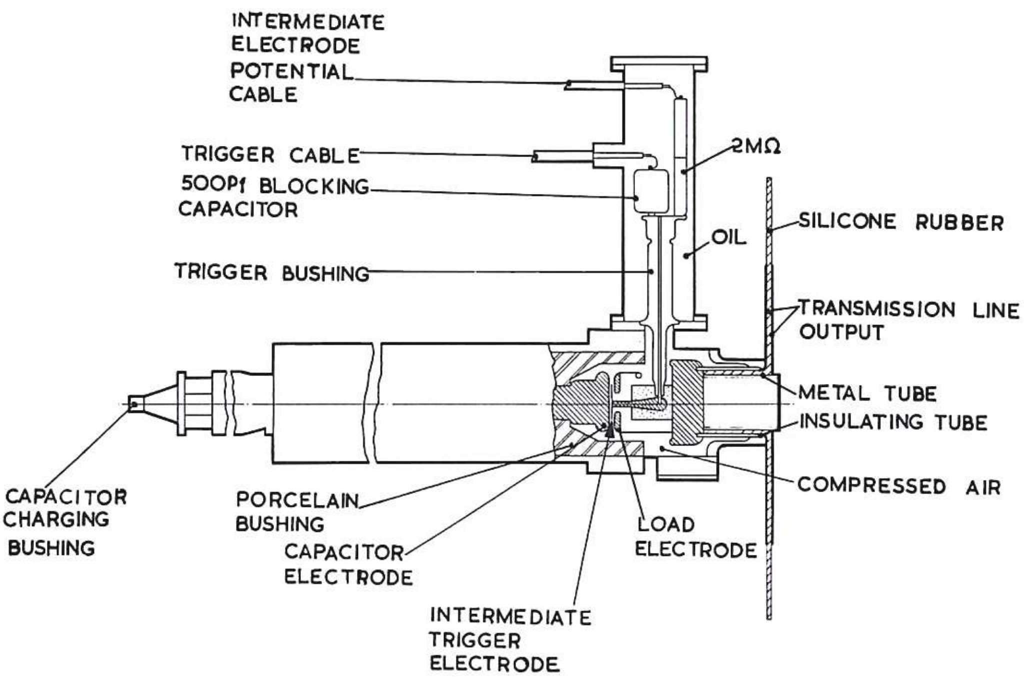

Fig.4(d) Start Switch, CUSIE (CLM-P81)

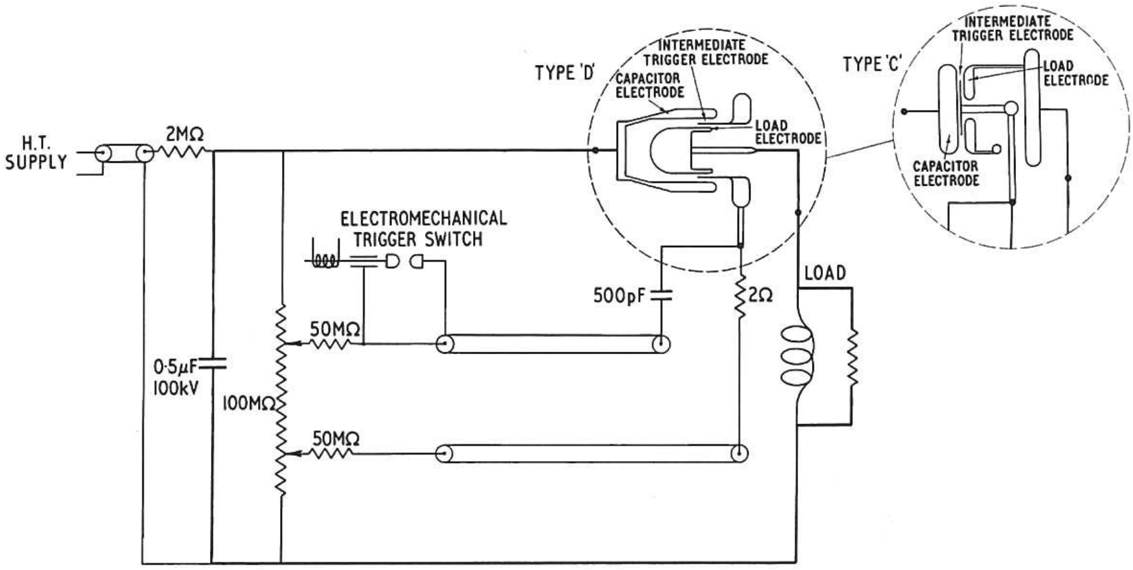

Fig.5 Test circuits for start switches (CLM-P81)

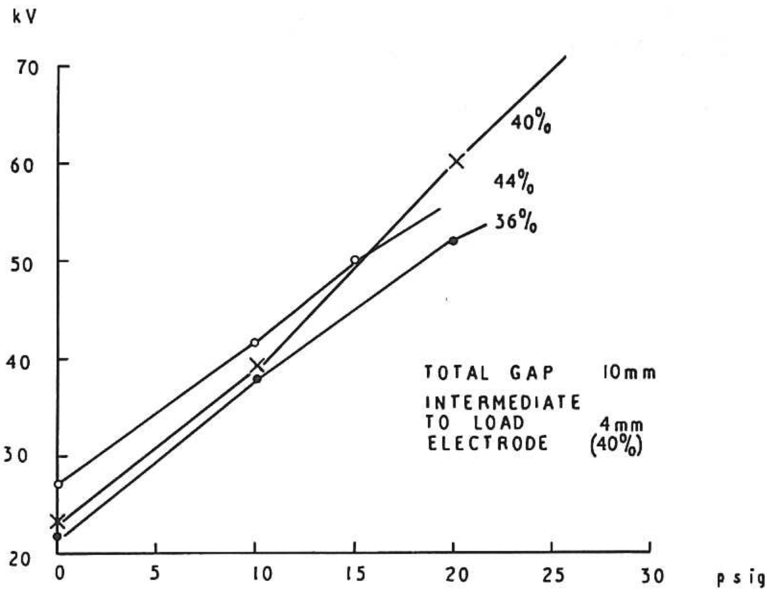

Fig.6 (CLM-P81)
Variation in static breakdown values with varying intermediate electrode potentials

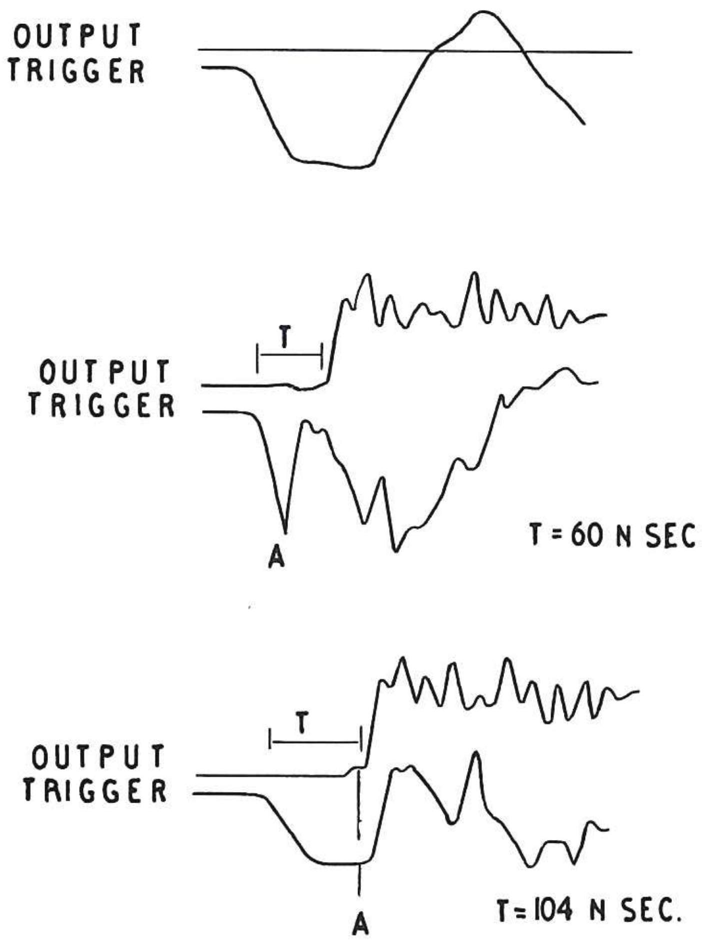

Fig.7 (CLM-P81)
Trigger and output waveforms for breakdown time measurements

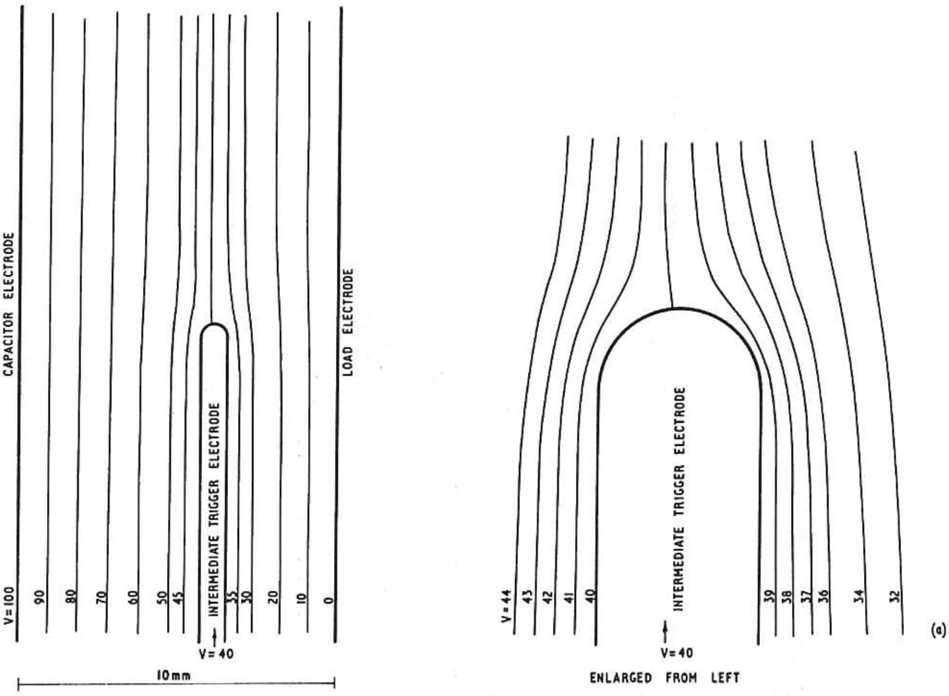

(a) Static condition. Intermediate electrode normal potential

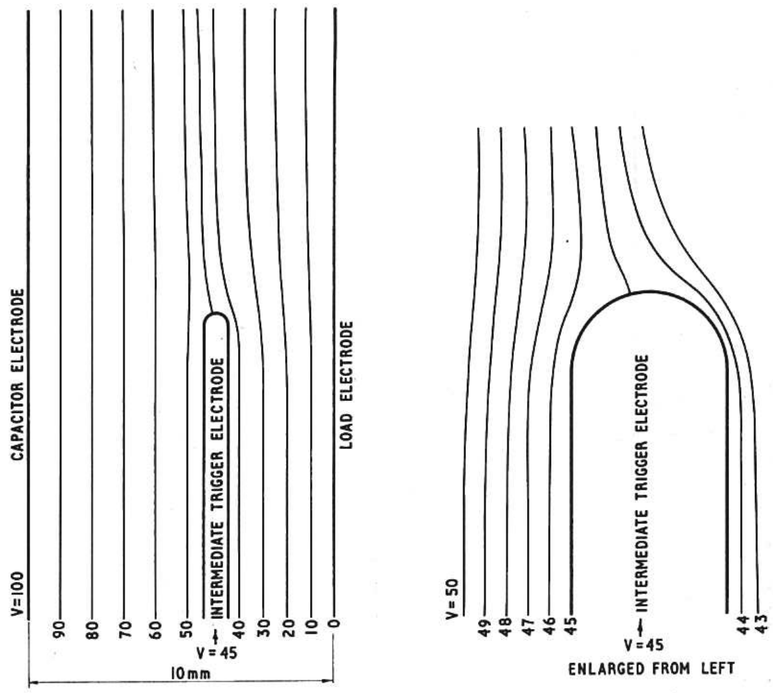

(b) Static condition. Intermediate electrode 5% above normal

Fig.8 Computed equipotential distribution (CLM-P81)

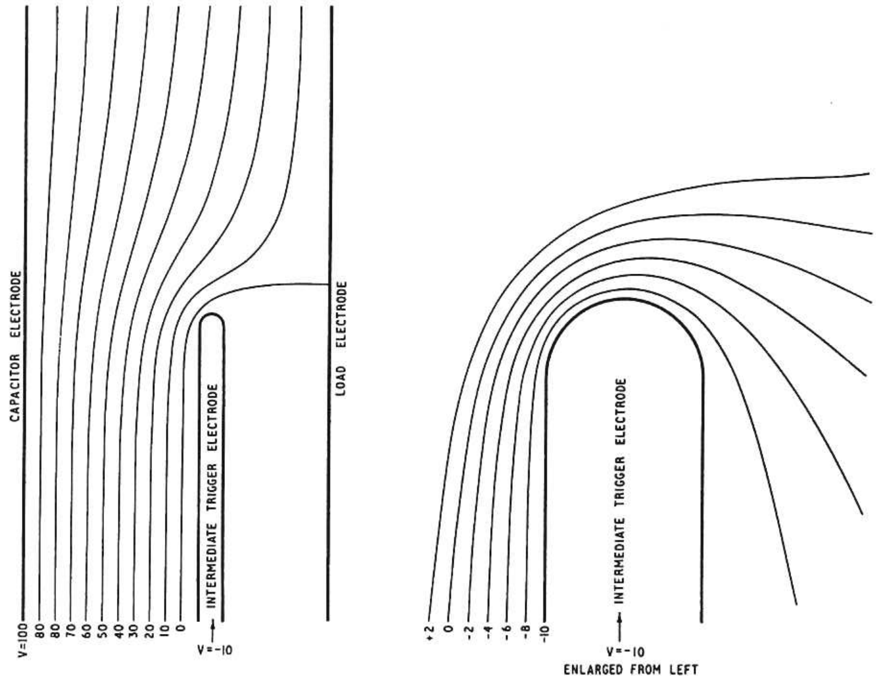

(c) Triggered 25%

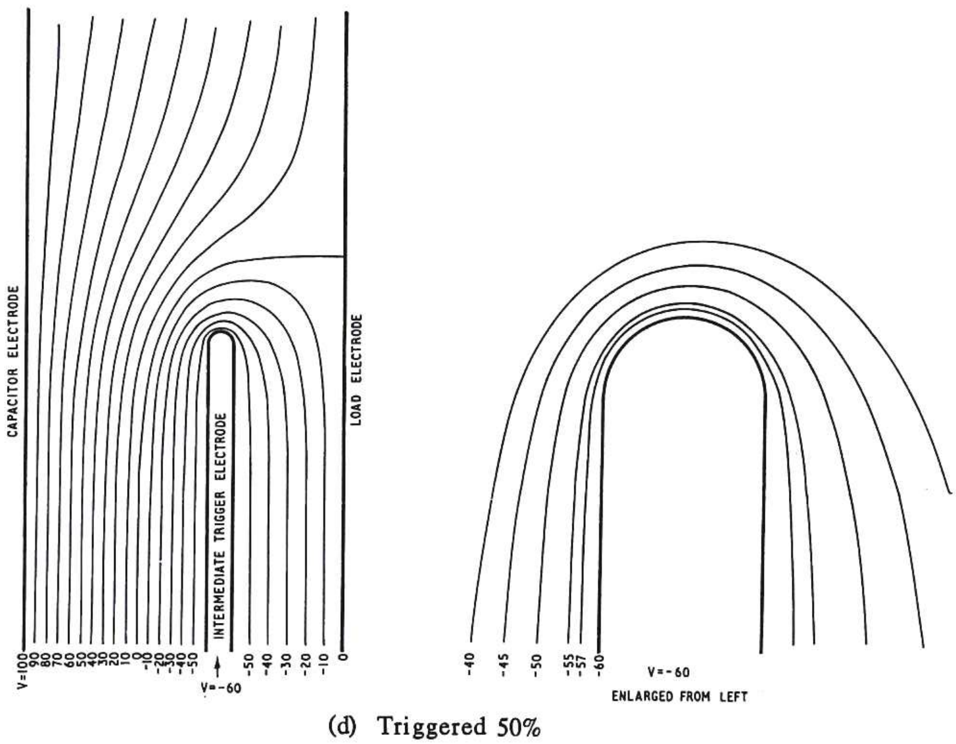

(d) Triggered 50%

Fig.8 (cont.) Computed equipotential distribution (CLM-P81)

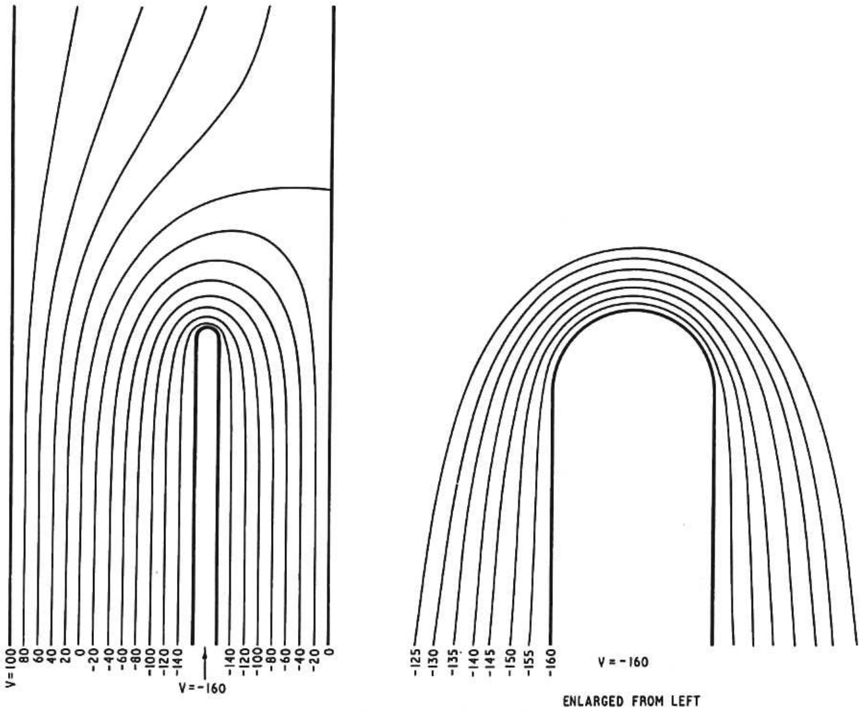

(e) Triggered 100%

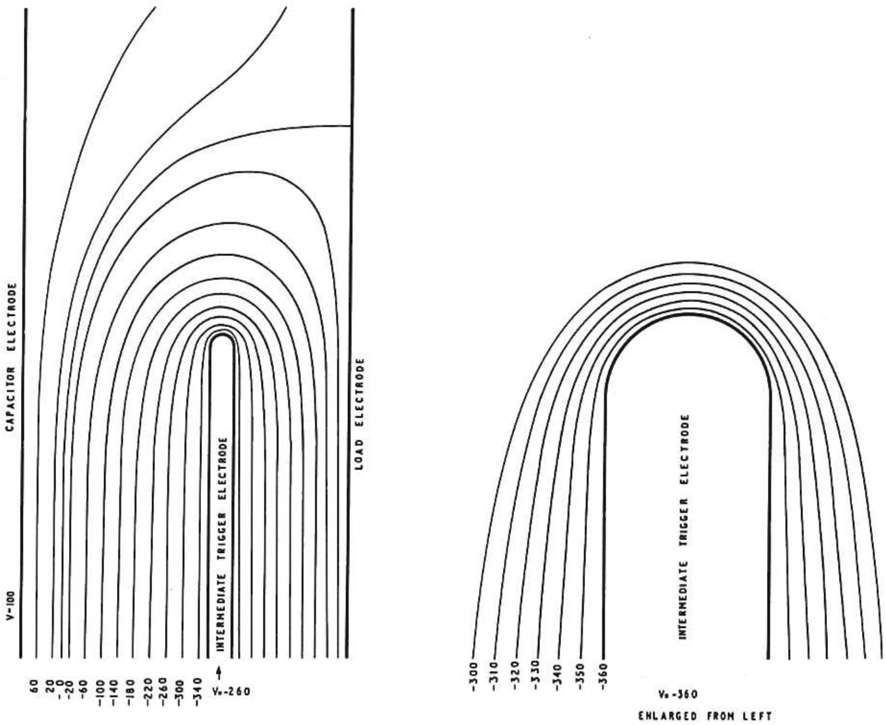

(f) Triggered 200%

Fig.8 (cont.) Computed equipotential distribution (CLM-P81)

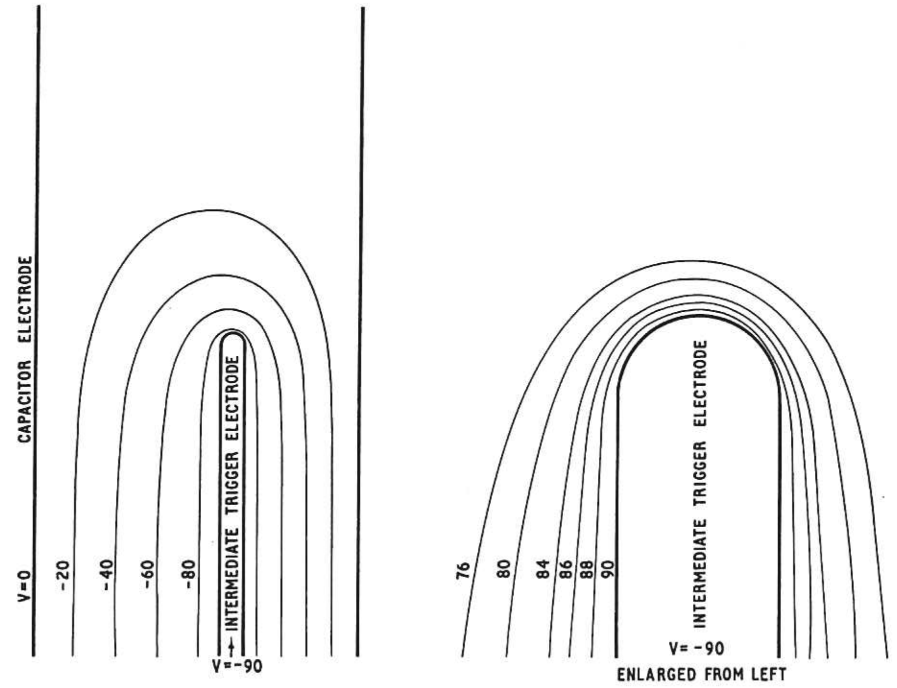

(g) Clamp condition + 45 kV trigger

Fig.8 (cont.) Computed equipotential distribution (CLM-P81)

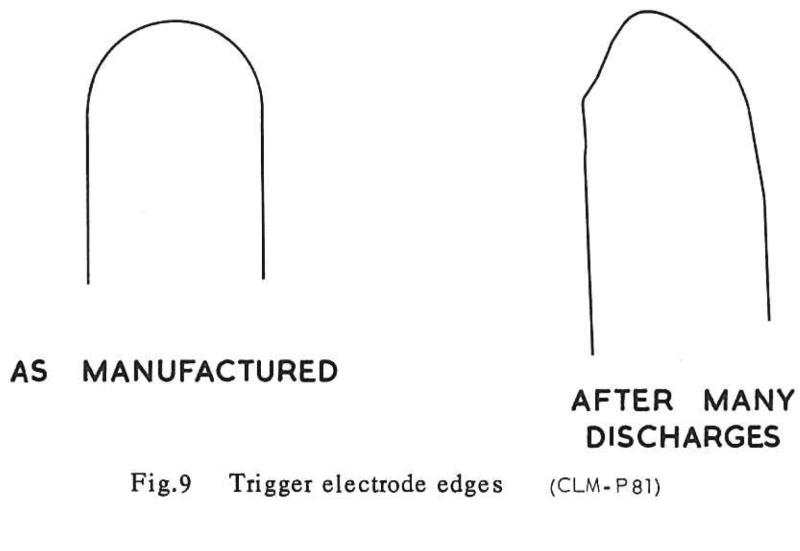

Fig.9 Trigger electrode edges (CLM-P81)

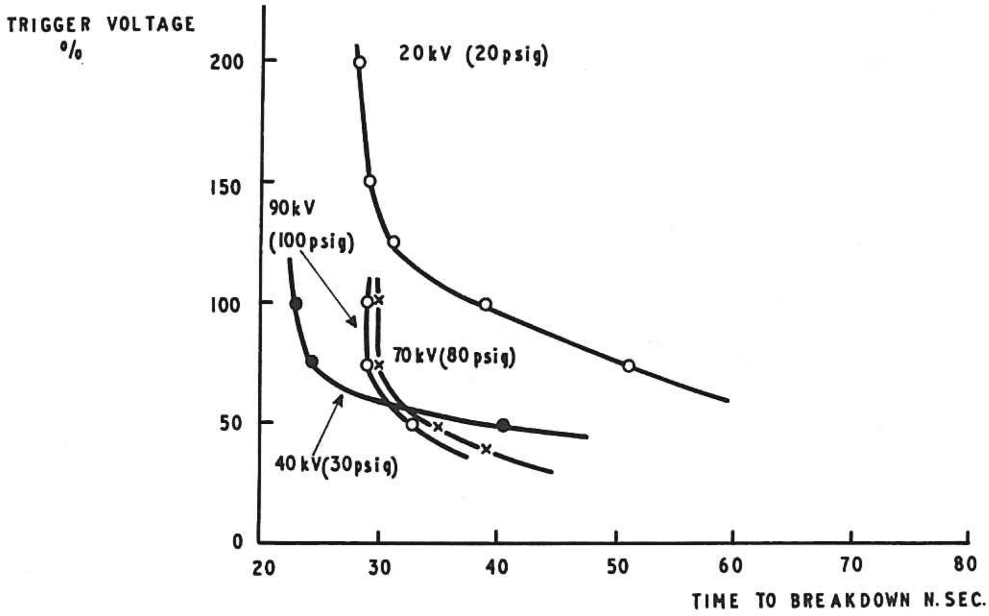

(a) Variable trigger voltage. Constant pressure and voltage across the switch

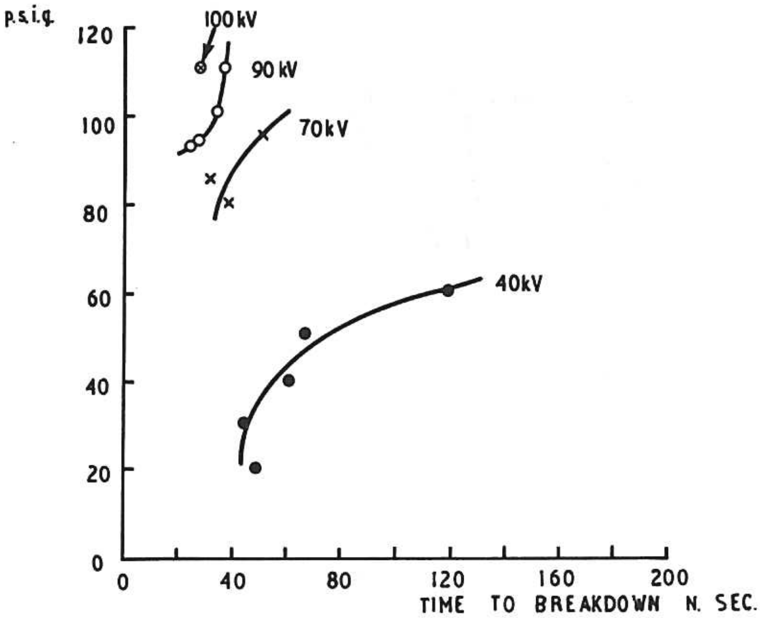

(b) Variable air pressure. Constant voltage across the switch and 50% trigger voltage

Fig.10 Breakdown time tests - type C (CLM-P81)

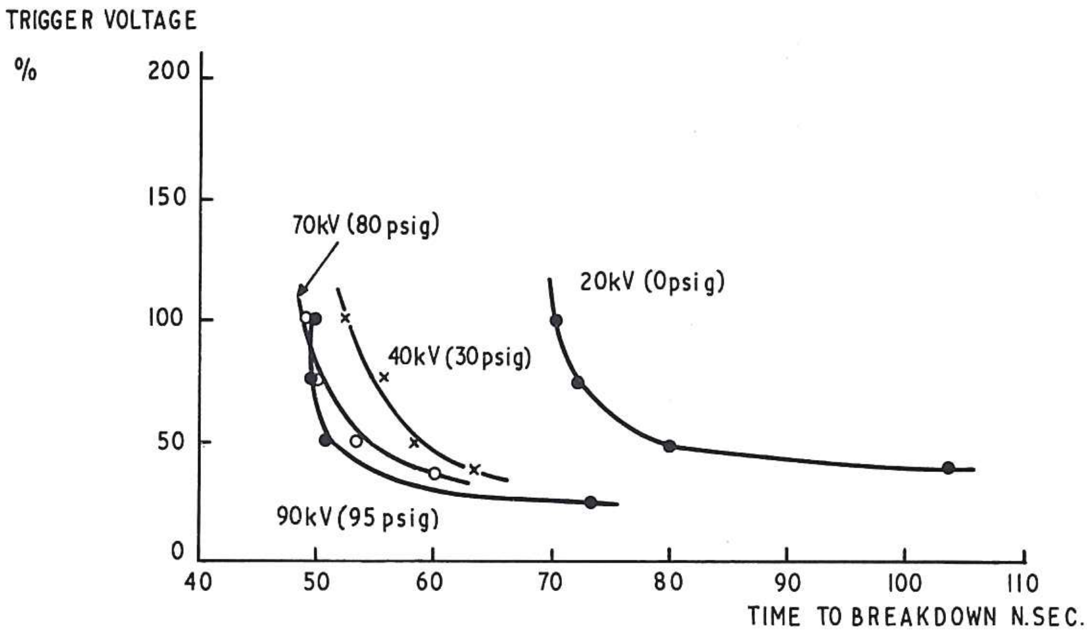

(a) Variable trigger voltage. Constant pressure and voltage across the switch

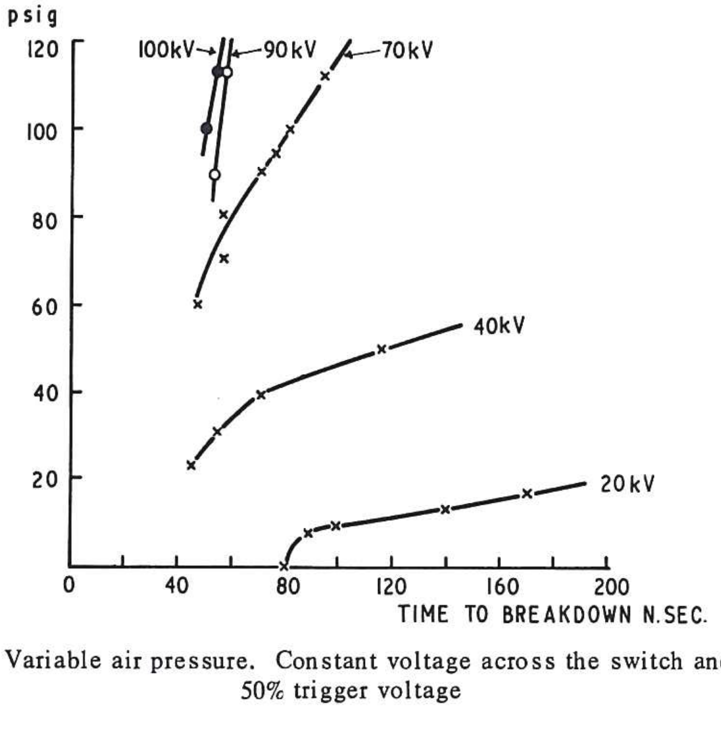

(b) Variable air pressure. Constant voltage across the switch and 50% trigger voltage

Fig.11 Breakdown time tests - type D (CLM-P81)

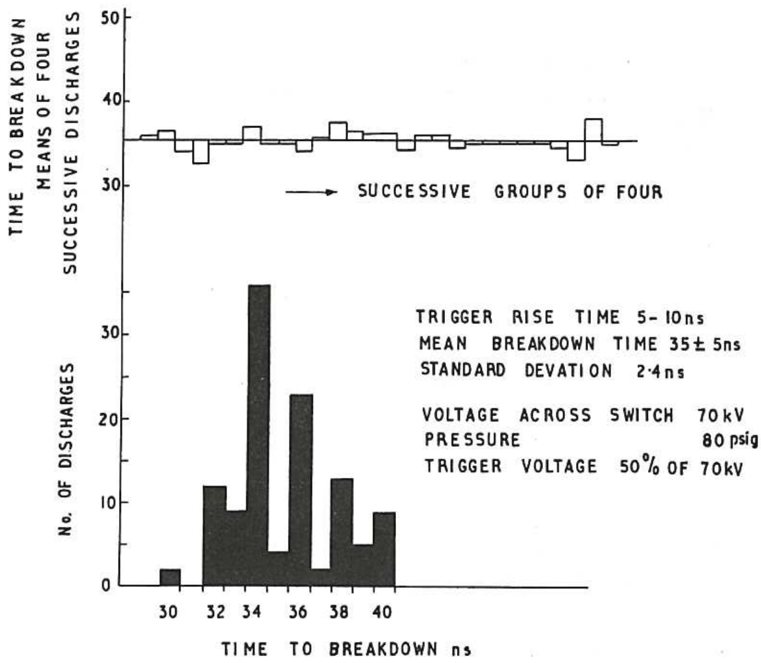

Fig.12 Jitter measurements - type C (CLM-P81)

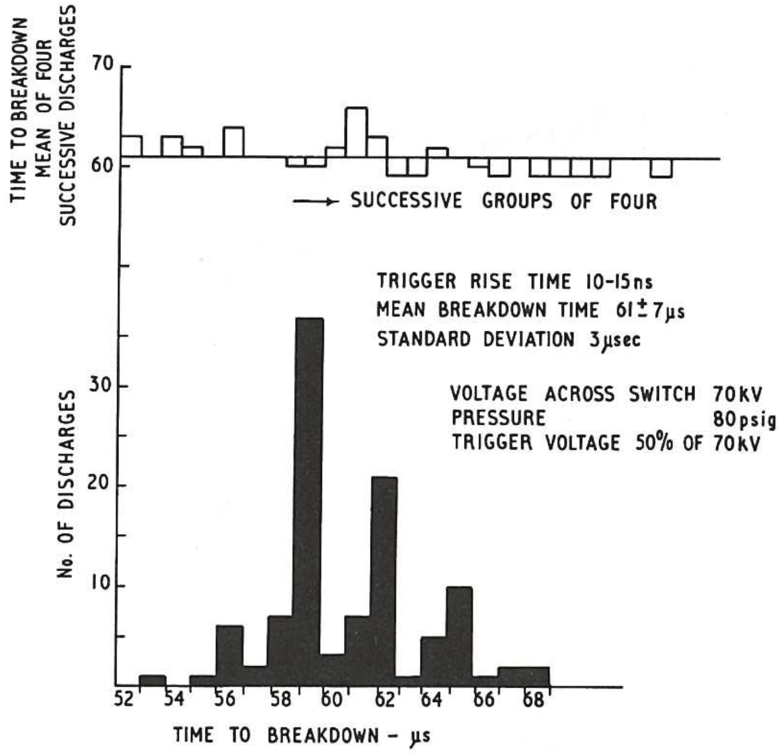

Fig.13 Jitter measurements - type D (CLM-P81)

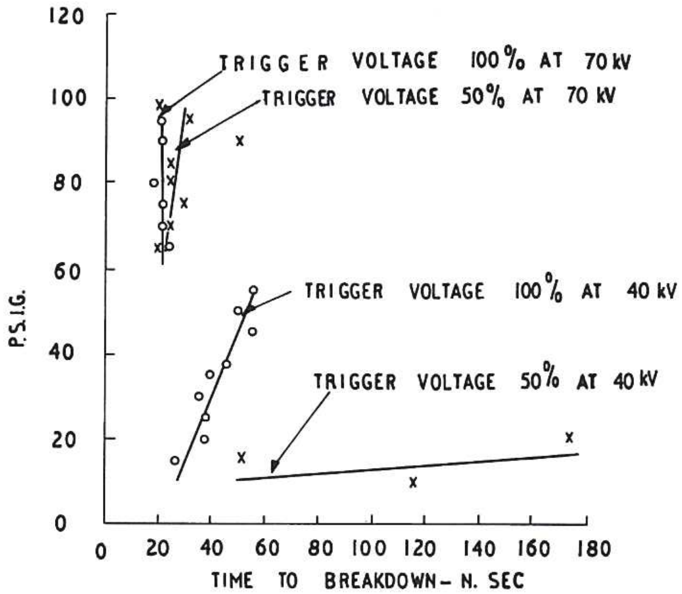

Fig.14 (CLM-P81)
Breakdown time tests - type C (negative polarity)

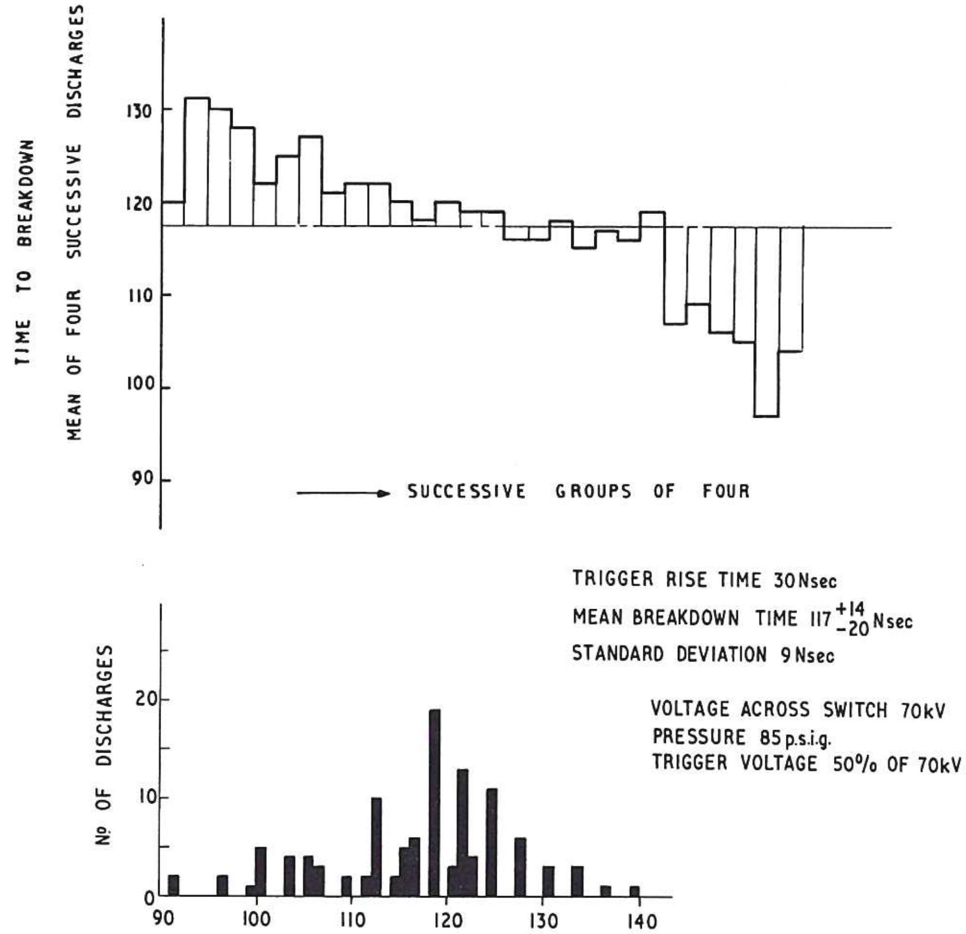

Fig.15 Jitter measurements Type C (long trigger rise) (CLM-P81)

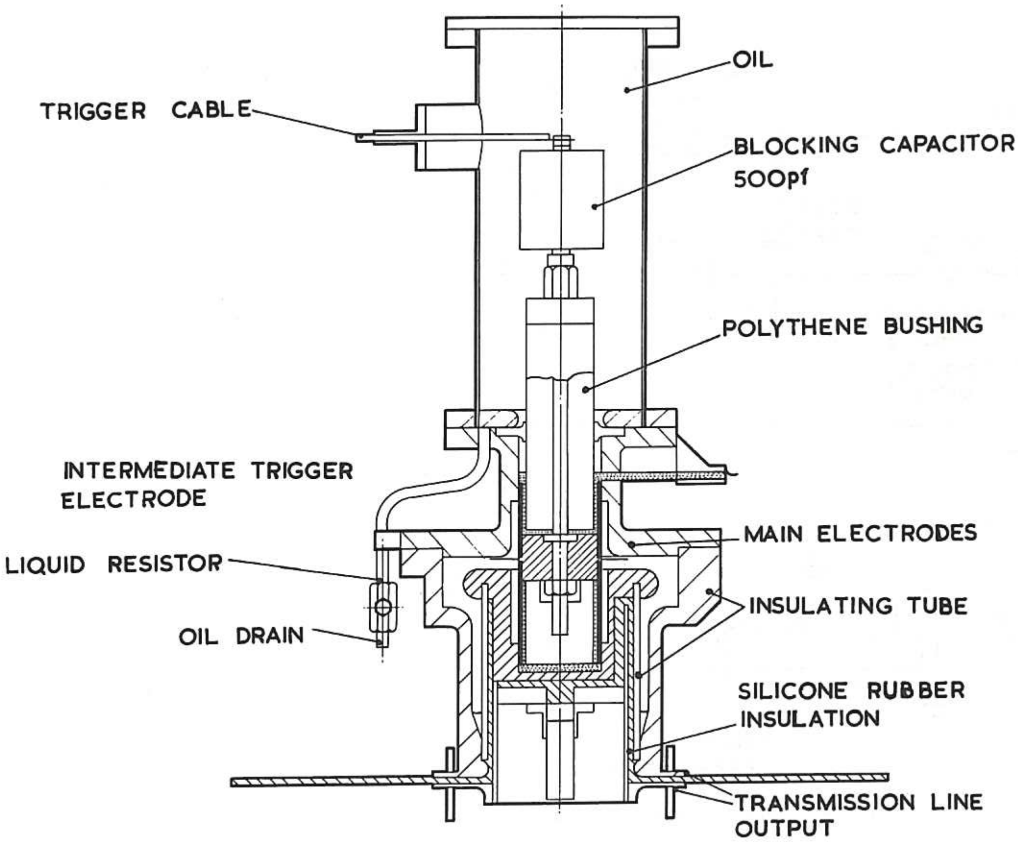

Fig.16 Divert switch (CLM-P81)

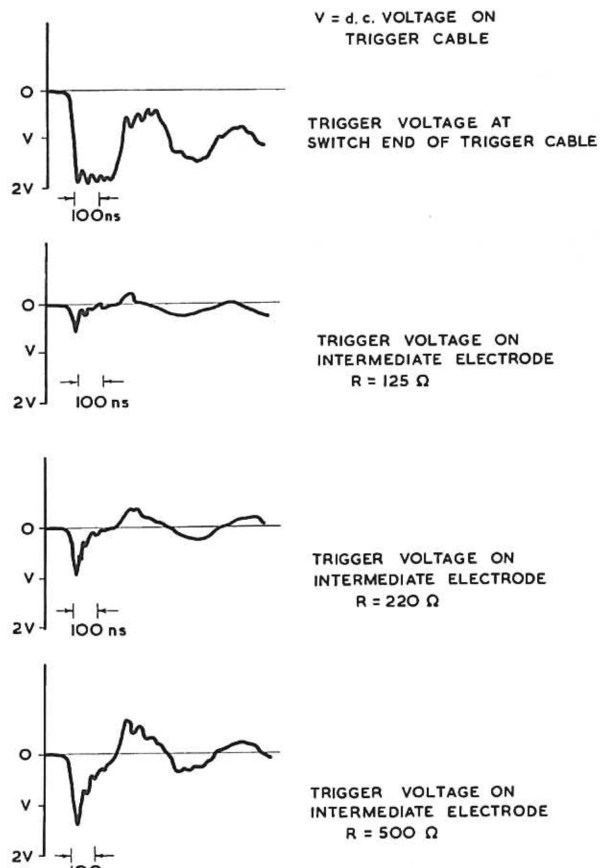

Fig.17 Divert switch trigger voltage waveforms (CLM-P81)

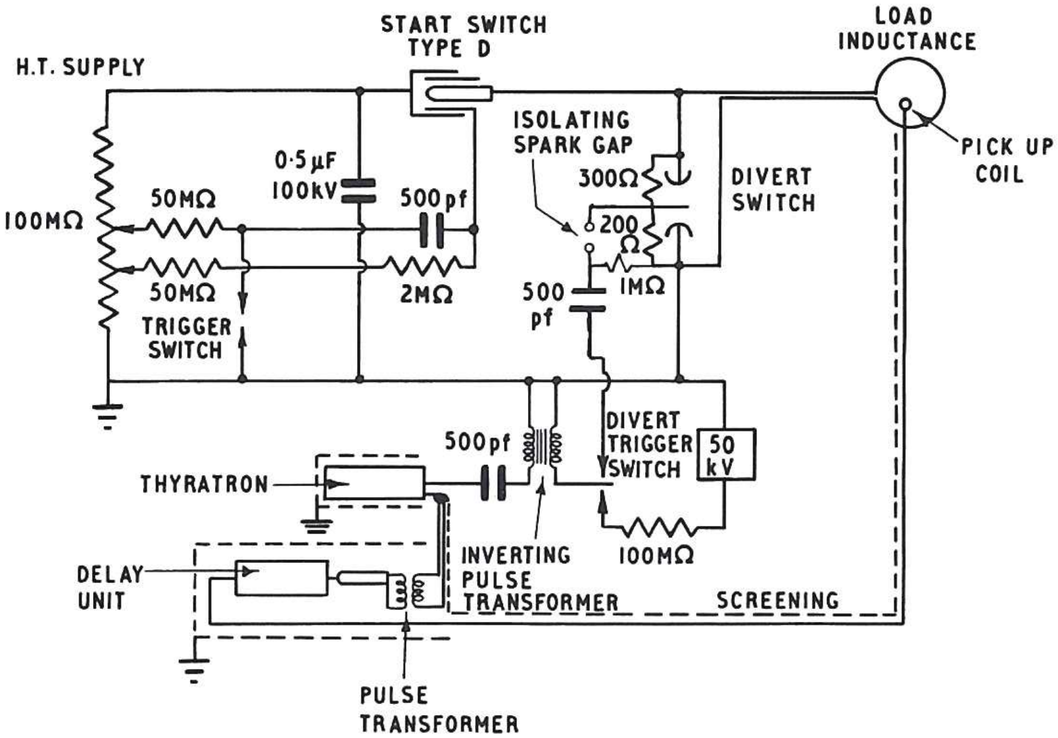

Fig.18 Divert switch test circuit (CLM-P81)

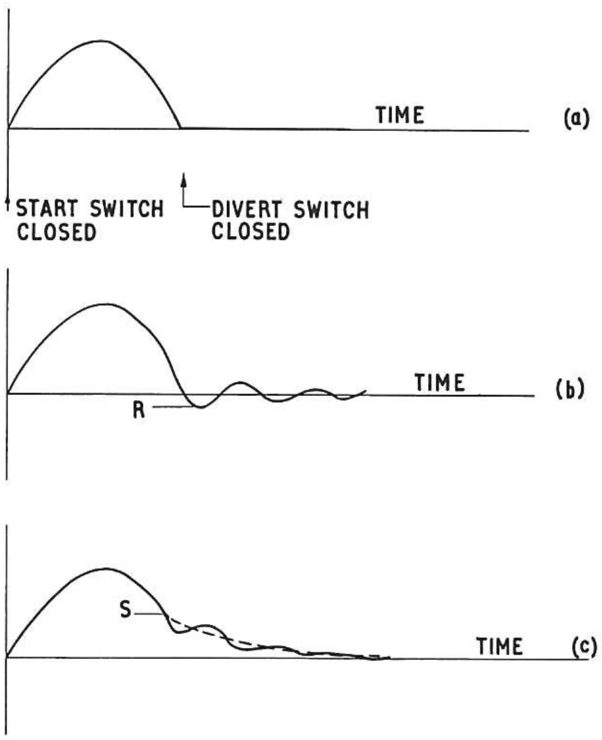

Fig.19 Divert current wavefoms (CLM-P81)

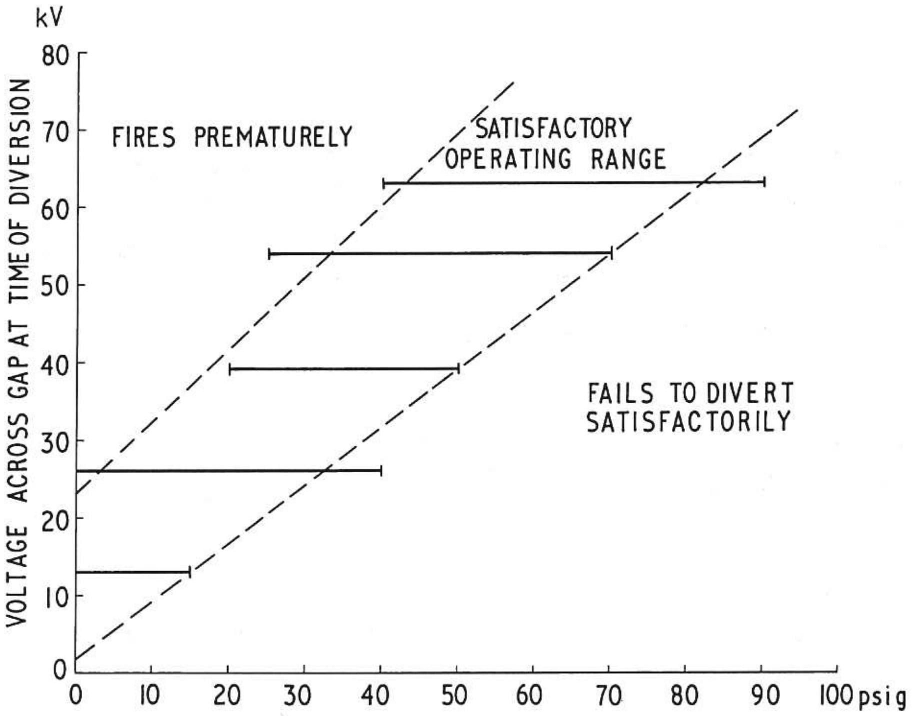

Fig.20 Operating range of divert switch (CLM-P81)

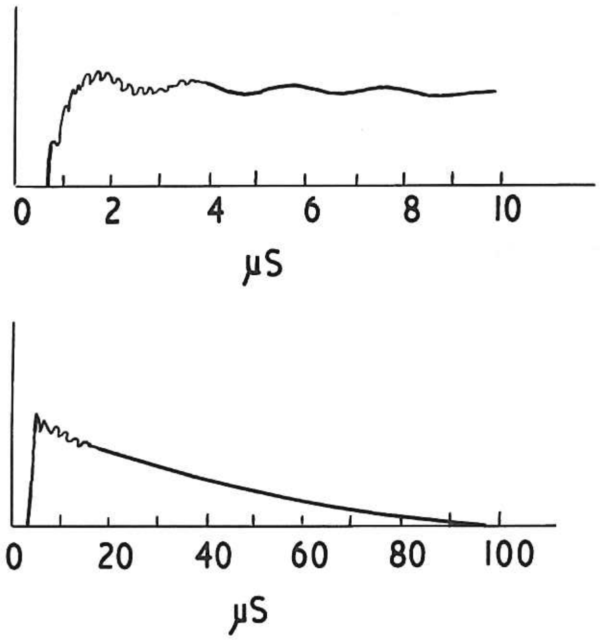

Fig.21 (CLM-P81)
A typical load current on clamping

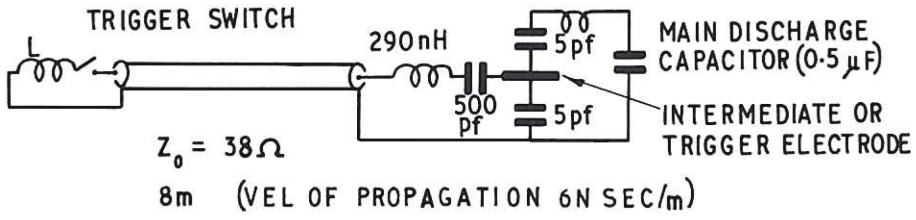

L 38nH NOMINAL TRIGGER RISE = 1n.SEC

L 380nH NOMINAL TRIGGER RISE = 10 n.SEC

L 1140nH NOMINAL TRIGGER RISE = 30 n.SEC

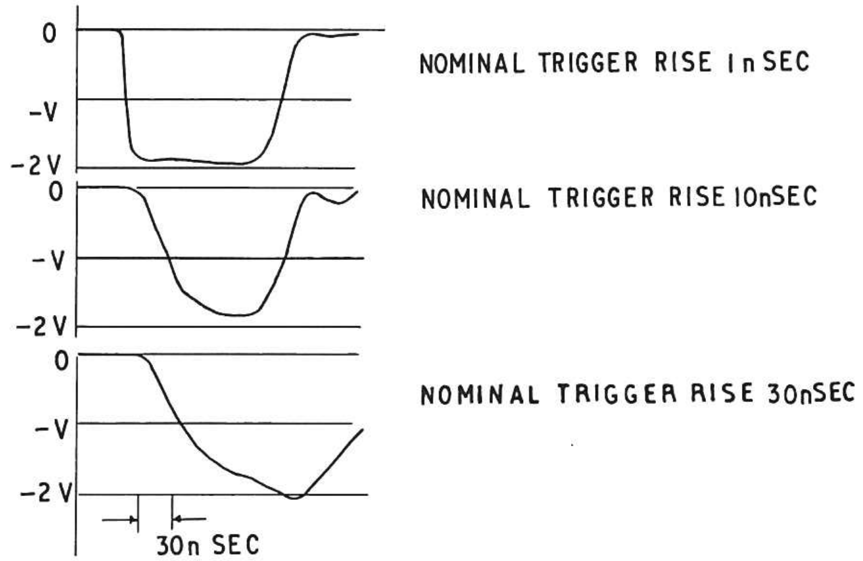

Fig.22 (CLM-P81)
Equivalent circuit of trigger input and wavefoms on intermediate electrode

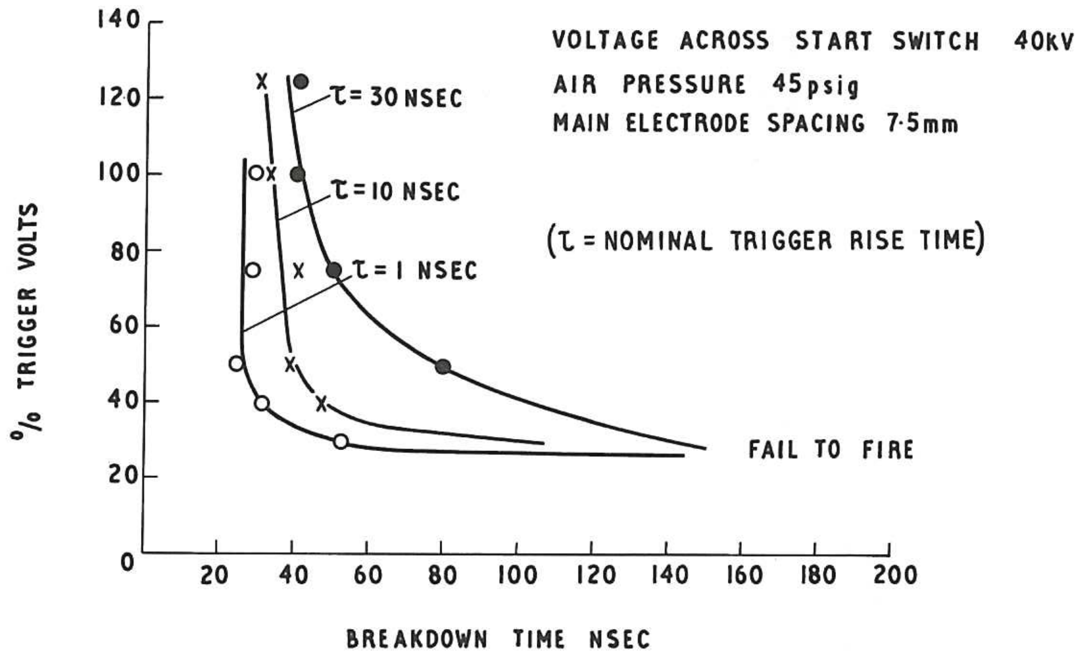

Fig.23 (CLM-P81)
Variation in breakdown time with trigger rise time

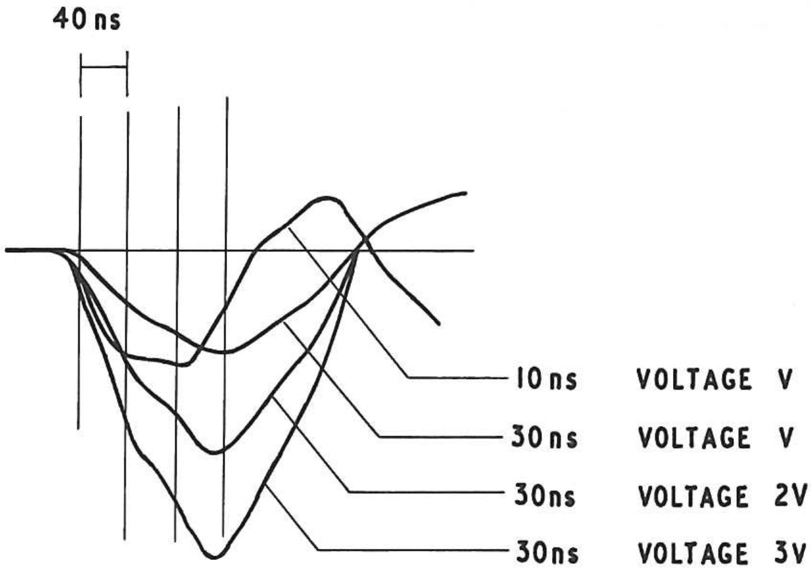

Fig.24 Expanded trigger wavefoms (CLM-P81)

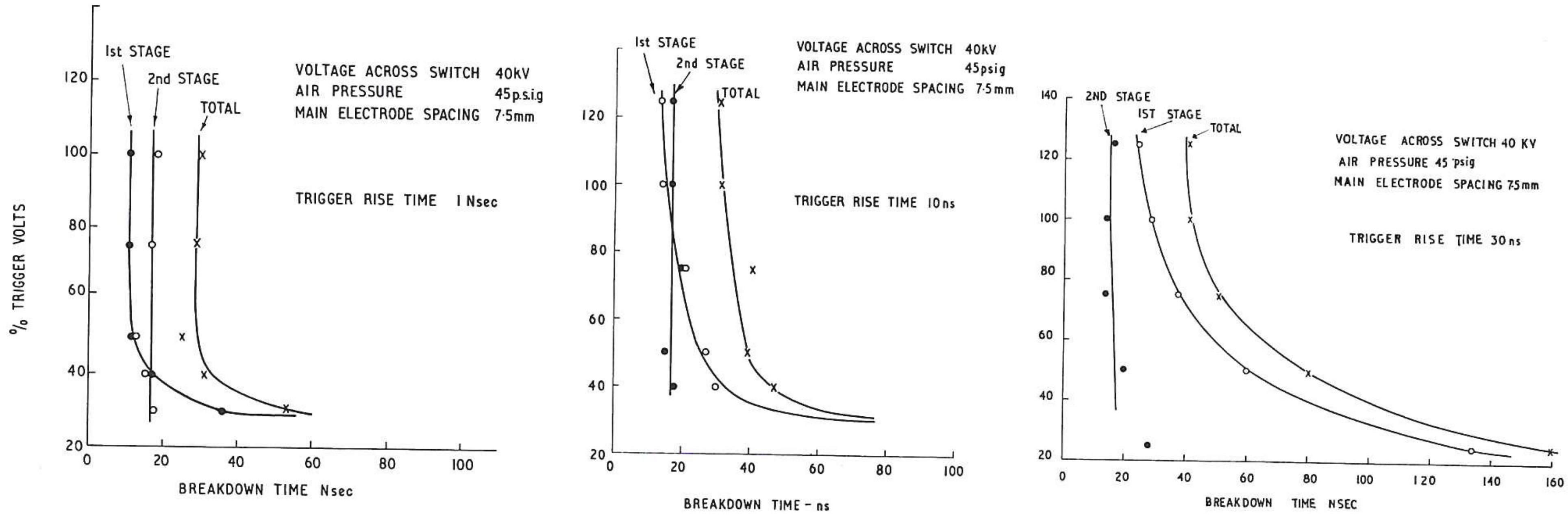

Fig.25 Breakdown times of first and second stages (CLM-P81)

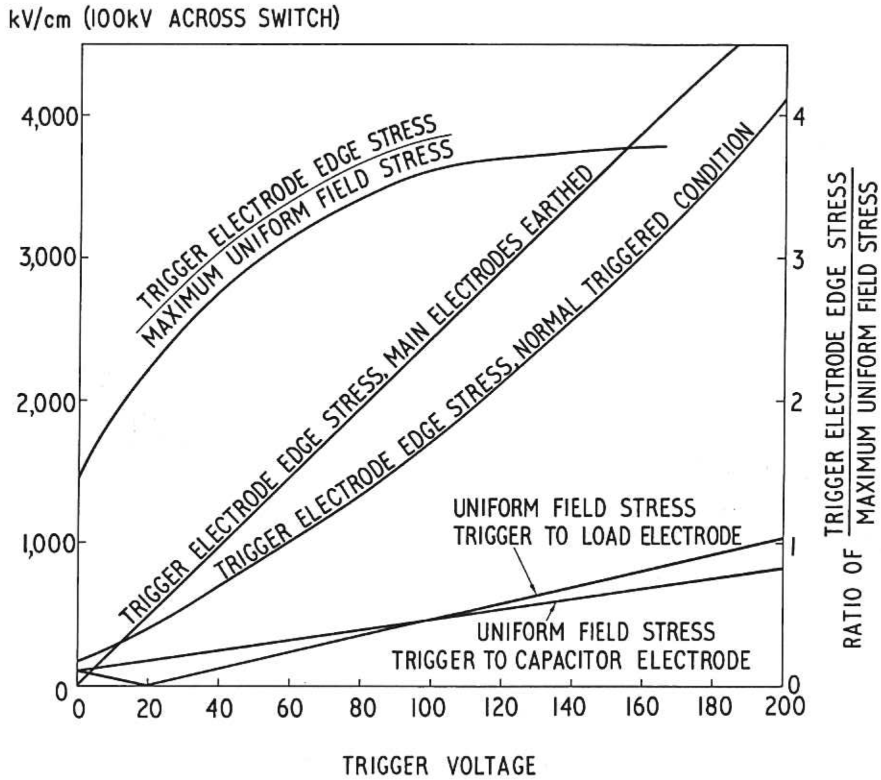

Fig.26 Computed electrode stresses (CLM-P81)

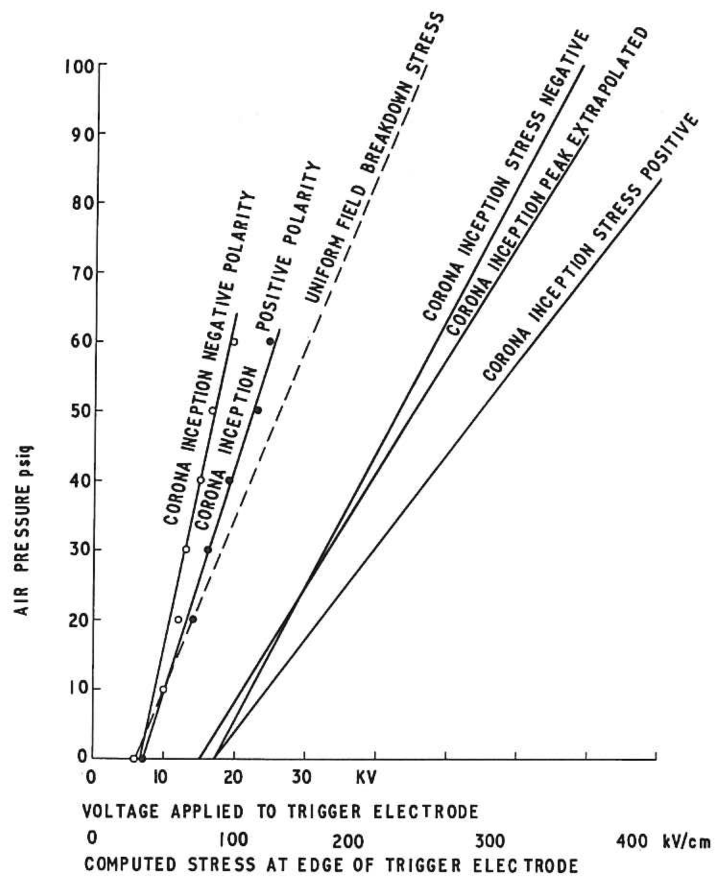

Fig.27 Corona inception measurements (CLM-P81)

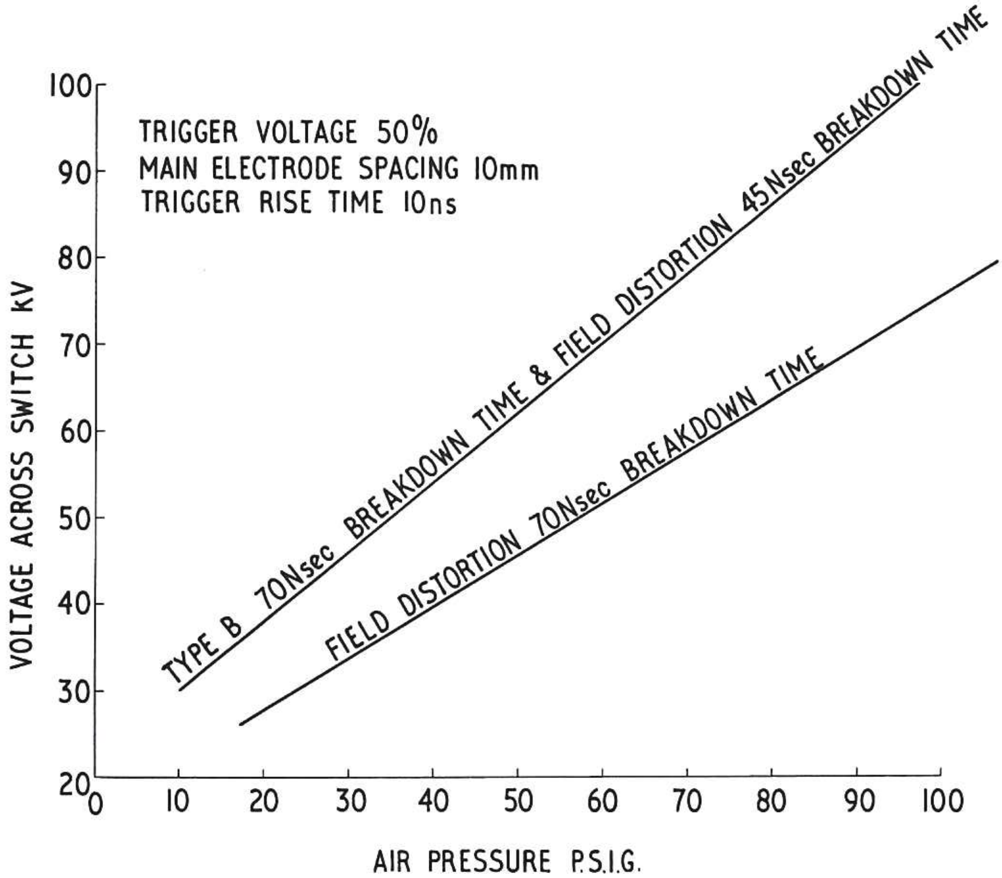

Fig.28 (CLM-P81)

Comparison of operating curves for type B and field distortion switches